FALKLAND ISLANDS DEPENDENCIES SURVEY

SCIENTIFIC REPORTS

No. 12

THE PETROLOGY OF GRAHAM LAND

II. THE ANDEAN GRANITE-GABBRO INTRUSIVE SUITE

By

R. J. ADIE, B.Sc., Ph.D.

Falkland Islands Dependencies Scientific Bureau
and
Mineralogy and Petrology Department,
University of Cambridge

LONDON: PUBLISHED FOR THE COLONIAL OFFICE
BY HER MAJESTY'S STATIONERY OFFICE: 1955

F.I.D.S. SCIENTIFIC REPORTS: No. 12

THE PETROLOGY OF GRAHAM LAND

II. THE ANDEAN GRANITE-GABBRO INTRUSIVE SUITE

By

RAYMOND J. ADIE,* B.Sc., Ph.D.

Falkland Islands Dependencies Scientific Bureau
and
Mineralogy and Petrology Department,
University of Cambridge

(Manuscript received 13th September, 1954)

ABSTRACT

As a result of a recent petrographic and geochemical re-investigation of the Andean granite–gabbro intrusive suite of Graham Land, based on material collected by the Falkland Islands Dependencies Survey during 1946 to 1950, it has been concluded that these rocks of Graham Land are all crystallisation-differentiation products of a common parental magma and form a normal calc-alkaline series, probably contemporaneous with that of the western Patagonian cordillera. Both the Graham Land and the Patagonian intrusive suites are assigned to a late Cretaceous or early Tertiary age.

Individual differential phases of this suite, which are subdivided geographically, are all described petrographically. Where available field and laboratory evidence is sufficient to warrant the correlation of geographical phases, this is given in tabular form. Attention is directed to the Terra Firma Islands layered gabbro intrusion which is described for the first time.

Twelve new complete chemical analyses of representative members of this series are presented together with their norms and other relevant information. The geochemical data, which are represented on triangular and linear variation diagrams, are critically reviewed and compared with those of other well-known calc-alkaline series. The relationship between the major and trace element concentrations is discussed and certain significant ratios are given in the tables. The approximate chemical composition of the supposed parental magma is also given.

Contamination of the parental magma by assimilation or palingenesis is believed to be of no great significance.

*Now at Research Department, Albright and Wilson Ltd., Oldbury, Birmingham.

CONTENTS

INTRODUCTION

THE Andean intrusive suite of Graham Land, closely comparable in chemistry and mineralogy with that of the South American Andes and Southern Patagonia, forms a definite series ranging in composition from basic gabbros to alkali-granites. As will be shown in the following pages of this report, these rocks are undoubtedly of common parentage and, apart from the rocks interpreted as basic accumulates, lie on the same line of liquid descent.

A cursory examination of the accompanying sketch map (Fig. 1), which illustrates the distribution of the Trinity Peninsula Series and the early Tertiary intrusives of Andean affinity, immediately reveals that the intrusives comprise about 80% of the Graham Land peninsula. In itself this is a most striking feature of the Andean intrusive suite. Without doubt these rocks can be regarded as being responsible for the very existence of the peninsula, having been emplaced both as gigantic batholiths and smaller boss-like masses. These intrusive bodies are not only confined to the core of the Graham Land peninsula but also form the greater part of the Palmer Archipelago and the Biscoe Islands off the northwest coast, and the western part of the South Shetland Islands.

In the course of their emplacement the intrusives have thrust aside the late Palaeozoic Trinity Peninsula Series sediments and have also invaded the extensive Jurassic rhyolite–andesite volcanic sequence. In view of this, it is significant to note that the Upper Jurassic to Lower Cretaceous sedimentary succession of Alexander Land is entirely free from igneous intrusives. However, field observations point to their possible presence beneath the sediments in the hinterland of this island, where the emplacement of a large batholithic mass has possibly been responsible for the large-scale eastward overthrusting of the Upper Jurassic/Lower Cretaceous sediments without actually traversing them. A small granite–diorite–gabbro complex, revealing the relations between the respective members of this series, occurs at the Eklund Islands in the east-west limb of King George VI Sound. Here the complex has suffered shearing, which is probably associated with the well-known tectonic disturbances in the Alexander Land sediments and which may be due to late stage batholithic emplacement in the near vicinity.

At about latitude 70° South, the widest part of the main Graham Land batholith gives rise to a high mountain chain of which the peaks have been estimated to be 12,000 ft. high (Ellsworth, 1937, p. 200). This chain continues in a southerly direction nearly to latitude 76° South, where it swings towards the southwest. Its furthest extremity extending across the Antarctic plateau is probably represented by "a solitary little range, symmetrically formed, with a central pyramid rising to 13,000 ft." (Ellsworth, 1937, p. 201).

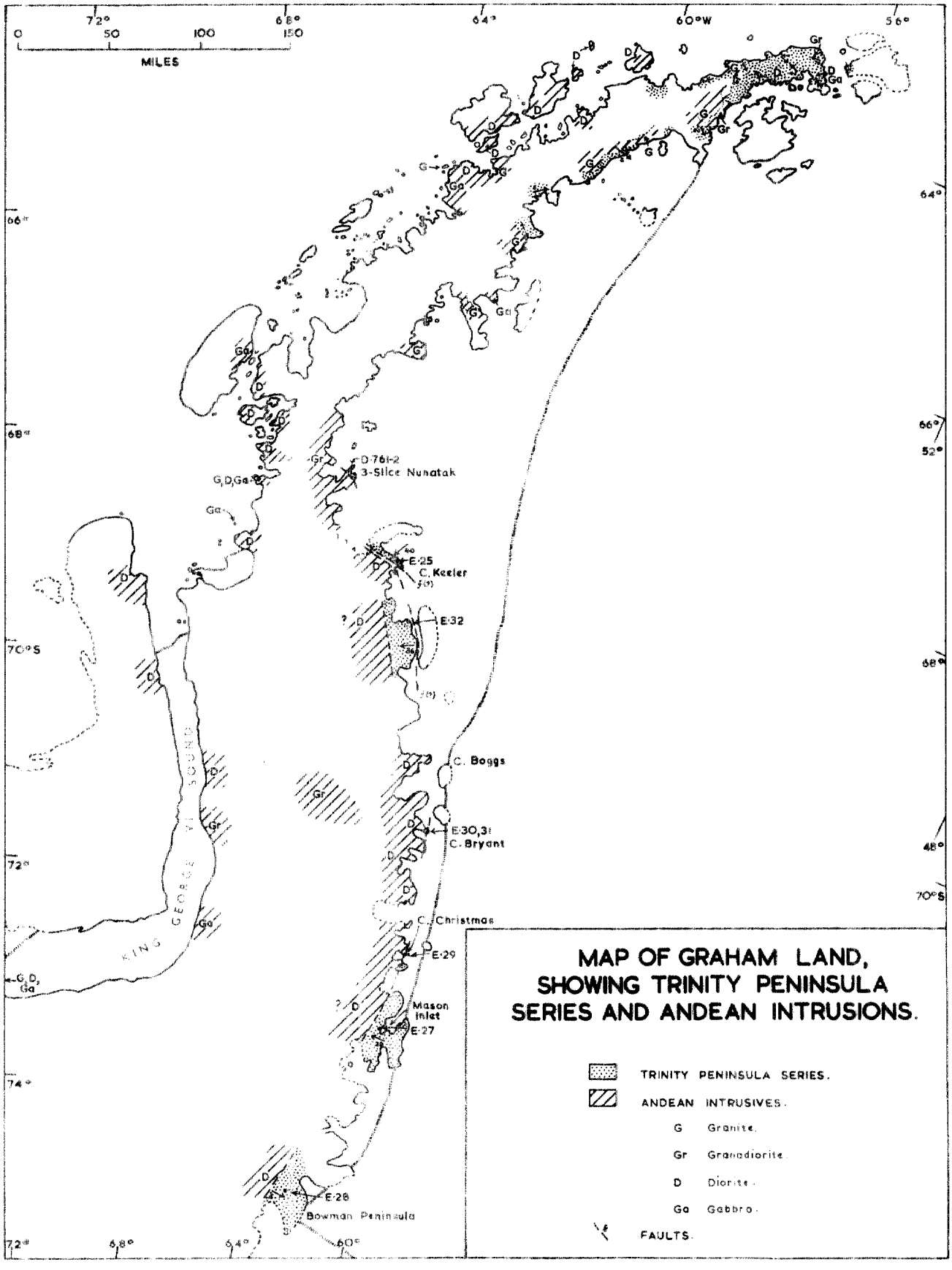

FIGURE 1

Map of Graham Land, showing the distribution of the Trinity Peninsula Series and the Andean intrusions.

In spite of their extensive occurrence in Graham Land, it is not yet possible to establish exactly the age of the Andean granite-gabbro intrusive suite. From an abundance of field data it is now clear that the Andean intrusives are younger than both the Trinity Peninsula Series and the Middle to Upper Jurassic sediments and volcanics, but nowhere has the relationship been established between the Lower or Upper Cretaceous sediments and the intrusives. Even in Alexander Land, where there is an uninterrupted sedimentary succession from the Upper Jurassic to the Lower Cretaceous, there is no definite evidence of intrusion by younger granites, diorites or gabbros of the Andean type.

Because there is no direct method of establishing the exact position of the Andean intrusive suite in the stratigraphy of Graham Land, it has been necessary to resort to an examination of the comparable stratigraphic succession of the western Patagonian cordillera in order to seek an answer to this problem. In the present case this approach to the problem of age relations is considered quite legitimate, since there is a direct connection between South America and Graham Land by way of the Scotia Arc.

In Patagonia, at both Cerro Payne and Mount Fitzroy, Hauthal (1898) has recorded Lower Cretaceous beds overlying granite laccoliths. The contact is certainly not sedimentary since these beds are traversed by granitic dykes associated with the laccoliths. In the area east of Cerro Payne definite Middle and Upper Cretaceous strata are intruded by Anden-diorite sheets, but the complete Tertiary succession, which is conformable upon the Cretaceous beds in other Patagonian localities, is entirely free from intrusions.

It may therefore be concluded that in Patagonia the Andean intrusive suite is perhaps very late Cretaceous or early Tertiary in age and that the Andean intrusive suite of Graham Land is probably contemporaneous with that of Patagonia.

The orogenic belt of the Antarctandes is considered to be contemporaneous with the Laramide foldings of the Andean cordillera and the Rocky Mountains of North America. Though compressional earth-movements probably began towards the end of the Cretaceous, they continued over a long period of time extending into the late Eocene and Lower Oligocene. The time of the batholithic intrusions was at a late stage in the orogeny, and after the main period of folding had subsided. The main fold axis is confined to the Graham Land peninsula itself with subsidiary foldings through the South Shetlands; the marginal Cretaceous areas of the James Ross Island group are relatively undisturbed and are only gently folded about an approximately north-south axis.

The work of Ferguson (1921), Holtedahl (1929), Barth & Holmsen (1939) and Jardine (Falkland Islands Dependencies Survey, 1950) in the South Shetland Islands has also shown that these intrusives are not especially confined to the main axis of the Antarctandes. Quite commonly they are found intruding the older Jurassic andesitic volcanics, but the younger Miocene-Pleistocene olivine-basalts and aqueous tuffs are free from intrusion. In this respect the South Shetlands may be regarded as being a subsidiary fold chain outside the main orogenic belt.

The Tertiary Andean intrusive suite of Graham Land and adjacent islands comprise the first Antarctic igneous rocks to be described in petrographic detail. Gourdon (1905, 1906, 1907, 1908, 1917 and 1919), Pelikan (1909), Sistek (1912), Bodman (1916), Holtedahl (1929), Barth & Holmsen (1939), Barth (1940), Knowles (1945) and Tyrrell (1921 and 1945) have made generous contributions to the petrography and petrology of the Andean intrusives of this area. It is, however, regrettable that in the past so little use has been made of the vast amount of data provided by the large number of available chemical analyses of these rocks. It is also unfortunate that nearly all the material described previously is no longer available for re-examination, because of its destruction during the two world wars or its loss through neglect.

Most of the earlier field work was carried out in the north of Graham Land, on the Danco and Graham Coasts, in the Palmer Archipelago and the Biscoe Islands. Since the inception of the Falkland Islands Dependencies Survey it has been possible to extend field operations to cover the whole of the east coast, the Marguerite Bay area, the Fallières Coast and the east coast of King George VI Sound. As a result of this recent work a more comprehensive idea of the field relations between the intrusives and the older rocks is now available. In addition, it has been possible to study in some detail the geochemistry of the batholiths themselves and the petrography of the various differentiated phases.

A correlation of the Andean intrusives for the whole of Graham Land is set out systematically in Table I, from which it is clear that in the majority of the areas examined there is repetition of the same order of intrusion. Of the regions described in detail, Trinity Peninsula and the Fallières Coast are the most important, since it is in these areas, which are marginal to the main body of the batholiths, that the differentiation process can be studied more clearly than elsewhere.

TABLE I

CORRELATION OF THE ANDEAN INTRUSIVES OF GRAHAM LAND

Trinity Peninsula	Nordenskjöld, King Oscar II, and Foyn Coasts	Bowman Coast and Southward to Latitude 75°S.	Palmer, Danco, Graham and Loubet Coasts; Palmer Archipelago and Biscoe Islands	Fallières Coast and Southward to Latitude 73°S. (Marguerite Bay Area)	Adelaide Island	Alexander Land	Eklund Islands
				Red Rock Ridge Granite			
				Cape Calmette and Camp Point Granites			
Cape Roquemaurel Granite Mount Reece Granite	Granite	Granite	Granite	= **Cape Berteaux Granite**			Granite (sheared)
Mount Bransfield Granodiorite	= **Cape Robinson Granodiorite**	Granodiorite	Granodiorite	(? Granodiorite)			
Blade Ridge Quartz-diorite	Diorite	Diorite	Diorite	= **Red Rock Ridge and Refuge Islets Quartz-diorite**	Diorite	(? Diorite)	Diorite
Tabarin Peninsula Diorite				= **Longridge Head Diorite**			
Nobby Nunatak Gabbro	Gabbro	Gabbro	Gabbro	= **Red Rock Ridge Gabbro Terra Firma Gabbro**	Gabbro		Gabbro
	(Gulliver Nunatak Intrusive Complex)						**(Intrusive Complex)**
		(see Knowles, 1945)					

The numbers given in the text in brackets, e.g. (D.337.1) and (E.29.1), refer to the official Station Lists of the Falkland Islands Dependencies Survey. The thin sections are housed in the Harker Collection, Mineralogy and Petrology Department, University of Cambridge.

The place-names used in this report will be found listed in the appendix together with the appropriate geographical positions. Those names given between inverted commas are not yet officially approved. The remainder will be found on the series of topographical maps on scales 1/100,000, 1/200,000 and 1/500,000 which are described in the Falkland Islands Dependencies Survey Scientific Report No. 1.

A. ANDEN-GRANITES

FAR less common than the ubiquitous quartz-diorites are the granites, which occur as small intrusive bodies in Trinity Peninsula, on the east and west coasts of Graham Land and in the Marguerite Bay area. The granites of the northwest coast and offshore islands are not re-examined in this report because they have been described already in some detail by Pelikan (1909), Gourdon (1908) and Bodman (1916).

In Graham Land it is possible to distinguish three distinct phases in the Anden-granites. The first is the coarse-grained pink biotite-granite of Cape Roquemaurel and Mount Reece, which is closely comparable to that found at Cape Berteaux in southern Marguerite Bay. The second type is identical in mineralogy to the first but is much finer-grained and found only at Cape Calmette and Camp Point, north of Neny Fjord, Marguerite Bay. The final magmatic phase is represented by the Red Rock Ridge granite, which occurs only in the Neny Fjord–Black Thumb Mountain area.

1. Cape Roquemaurel and Mount Reece Granites

Tyrrell (1945) has already described a biotite-granite from Cape Roquemaurel (Station 1490), but since his description is somewhat brief this granite will be described in more detail here.

At both Cape Roquemaurel and Mount Reece this granite intrudes the Trinity Peninsula Series but so far only the general thermal metamorphic effects have been studied (The Petrology of Graham Land: III. Metamorphic Rocks of the Trinity Peninsula Series). In the hand specimen the Cape Roquemaurel (D.337.1) and Mount Reece (D.375.2) granites are medium- to coarse-grained and have a pale pink colour. The only ferro-magnesian mineral distinguishable in the hand specimen is biotite, which occurs as small

TABLE II

MODAL ANALYSES OF BIOTITE-GRANITES

	D.337.1	D.375.2	D.747.10	D.754.2	D.754.3
Quartz	28.9	33.9	35.4	33.2	28.5
Orthoclase	23.6	22.3	39.1	32.5	28.7
Plagioclase	43.4	36.2	20.1	18.2	39.6
Muscovite					0.9
Biotite	3.0	7.5	4.8	8.1	1.1
Chlorite	1.0				
Hornblende	0.1	0.1	*	*	0.2
Iron ore	*	*	0.6	0.7	0.1
Apatite	*	*	*	*	*
Sericite	*	*	-	-	-
Epidote				7.1	0.9
Calcite				0.2	-
Zircon	*	*	*	*	*
Plagioclase Composition	$Ab_{75}An_{25}$†	$Ab_{90}An_{10}$†	$Ab_{90}An_{10}$	$Ab_{91}An_{9}$	$Ab_{92}An_{8}$

*Indicates present but not estimated.
†Plagioclases zoned.

D.337.1 Biotite-granite; Cape Roquemaurel.
D.375.2 Biotite-granite; Mount Reece.
D.747.10 Biotite-granite; erratic from Evensen Nunatak
D.754.2, D.754.3 Biotite-granite; Gulliver Nunatak.

scattered flakes throughout the rock. In thin section the rock has a coarse granitic texture and consists mainly of quartz, orthoclase and plagioclase with accessory biotite and a little hornblende (Table II). The orthoclase is seldom microperthitic and is frequently dusty with alteration products. The plagioclase has a composition of approximately $Ab_{90}An_{10}$. Sometimes it shows good chequer-twinning though generally twinning is according to the Carlsbad/albite law. Zoning, which is particularly marked in the plagioclases of the quartz-diorites and mica-diorites, is rare in the granites but it has been noticed. In these cases the more acid rims are $Ab_{95}An_5$ whereas the cores have a composition of $Ab_{85}An_{15}$. Alteration to saussurite is common, being particularly pronounced in the more basic cores of the zoned plagioclases. The interstitial allotriomorphic quartz is markedly dusty with inclusions but it never shows undulating extinction or strain shadows as is the case with some of the older granites. Biotite, with pleochroism scheme $\alpha = \beta =$ pale straw and $\gamma =$ deep brown, occurs as small accessory flakes with abundant scattered zircon inclusions and is often altered to chlorite. In addition to biotite minute common hornblende crystals are found throughout the rock. Other accessories include apatite and zircon. Sphene is markedly absent. As an alteration product epidote is known to occur in addition to saussurite and sericite in the plagioclase felspar.

The pink granites of Cape Berteaux, Moraine Cove and the Eklund Islands are both macroscopically and microscopically identical to the Cape Roquemaurel and Mount Reece granites and may therefore be tentatively correlated with them. Modal analyses of the biotite-granites are set out in Table II, where they are compared with similar granites from Gulliver Nunatak on the east coast of Graham Land.

Although it is often difficult to differentiate between hand specimens of the old "Coarse Pink Granites" and the younger granites, microscopic examination of thin sections reveals several striking differences. For example, the older granites are invariably rich in microperthitic potash-felspar, whereas the younger ones contain very nearly pure orthoclase; hornblende never appears in the older granites; sphene is limited to the older granites alone; and the quartz of the older granites exhibits a purplish colour in the hand specimen, whereas it is milk-white in the younger granites.

At the Eklund Islands the biotite-granite is certainly the youngest member of the igneous complex, intruding both the quartz-diorites and the gabbros. Such an assemblage is seldom found elsewhere in Graham Land but it is repeated almost identically in the Gulliver Nunatak igneous complex on the King Oscar II Coast. The order of intrusion is always from basic to acid in these smaller complexes. Apart from late aplitic and pegmatitic dykes, no close relative of the Red Rock Ridge granite has been found so far except in the Neny Fjord–Black Thumb Mountain area of Marguerite Bay.

2. Cape Calmette and Camp Point Granites

The granite which occurs in both these areas is medium- to fine-grained in texture and is mineralogically identical to that already described from the Cape Roquemaurel area. The only distinguishing feature, apart from the finer texture, is the fact that small more basic xenoliths occur in this granite on the northern side of Camp Point. They are seldom found in the Cape Calmette granite.

3. Red Rock Ridge Granite

The type locality for the Red Rock Ridge granite is Red Rock Ridge itself, but it also extends over the north-eastern side and head of Neny Fjord, the Black Thumb Mountain area and southern Millerand Island. Two distinct facies of this granite, respectively red and grey in colour, have been distinguished in the field. The former is by far the more common and represents the type material. The grey facies occurs only in the Black Thumb Mountain area and on the rocky promontory to the north.

In the hand specimen the Red Rock Ridge granite possesses a characteristic drusy appearance and a pale reddish-pink colour, which is more pronounced in the parent mass than in the hand specimen. Some of the druses are filled with hydrothermal chlorite, beautifully terminated quartz crystals, calcite and limonite. Nichols (1948) states that this granite carries molybdenite, but so far it has not been recorded in any of the material under examination. Since this granite is regarded as belonging to a very late magmatic stage, it is quite within reason to expect molybdenite mineralisation.

In thin section the Red Rock Ridge granite is very easily distinguished from the other granites by its medium grain size and characteristic myrmekitic texture (Plate Ib). It consists entirely of a symplectic intergrowth of quartz, orthoclase and oligoclase-albite. The plagioclase is usually albite-twinned and altered to saussurite in patches; there is never any zoning. The greater part of the orthoclase is slightly altered to kaolin and other degradation products. In some of the thin sections the orthoclase is slightly perthitic with small clear albite lamellae. Around both the orthoclase and perthite, quartz forms a vermicular intergrowth with orthoclase, imparting to the rock its typical myrmekitic texture.

Dark minerals are uncommon but a little accessory biotite with pleochroism in straw and dark brown makes its appearance in small fresh flakes. Apart from rare apatite and zircon, magnetite is the only other accessory mineral. It always occurs as small grains occupying an intergranular position. In the red facies

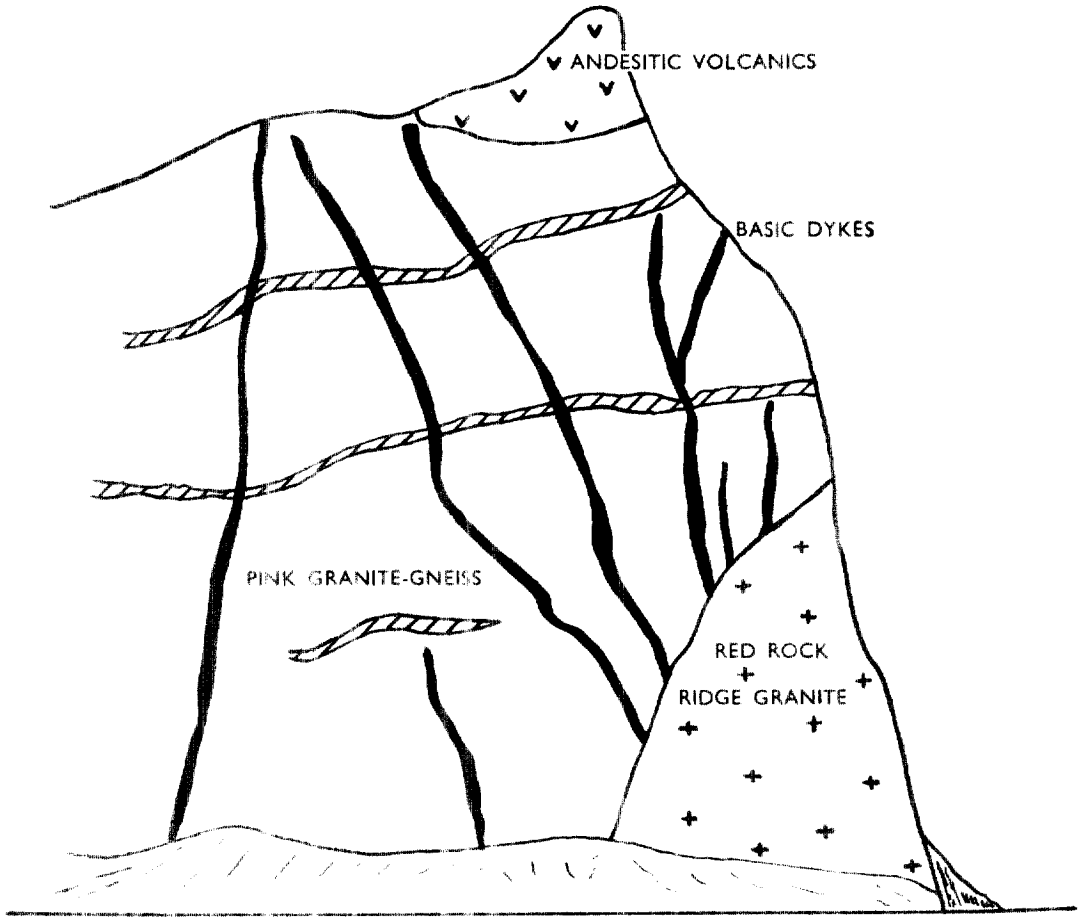

FIGURE 2

The Red Rock Ridge granite truncating basic dykes which invade the Basement Complex pink granite-gneisses on the west coast of Millerand Island. The andesitic volcanics, resting directly on the granite-gneisses here, are allied to the basic dykes in the gneisses.

the magnetite is invariably altered to limonite, which imparts a reddish colour to some of the potash-felspars. On the other hand, the grey facies exhibits none of these alteration products. Sphene, which is so characteristic of the older "Coarse Pink Granite", is notably absent here.

At Black Thumb Mountain the field relations show clearly that the Red Rock Ridge granite is younger than the "Coarse Pink Granite" which it intrudes with a sharp contact showing a narrow finer-grained

selvage to the Red Rock Ridge granite. At Millerand Island this same granite has intruded the Basement Complex (Fig. 2) in a boss-like fashion. On Red Rock Ridge itself the red granite is traversed by numerous felsitic dykes, along the contacts of which the red granite is considerably altered. Though the granite has preserved its typical myrmekitic texture, the plagioclase is almost entirely replaced by granular epidote and clino-zoisite. The orthoclase is also heavily altered.

B. GRANODIORITES

GRANODIORITES, which from their field relations are also presumed to belong to the Andean intrusive suite, occur in the Mount Bransfield area in close association with biotite-granites similar to those of Cape Roquemaurel. They are extremely coarse-grained, greyish in colour and possess a significant amount of both biotite and hornblende in addition to quartz, oligoclase and orthoclase. The plagioclase in the granodiorites is much more basic than that of the biotite-granites, having a composition of $Ab_{74}An_{26}$, and often shows zoning. The orthoclase is always perthitic, containing albitic lamellae that are totally free from saussuritisation. The orthoclase itself is invariably highly altered. Quartz, dusty with inclusions, is interstitial and though it is frequently cracked, rarely shows any signs of strain. The biotite occurs in small clots together with hornblende and both these minerals are slightly altered. The accessories include apatite, zircon and an abundance of iron ore (ilmenite and magnetite). Sphene is sometimes found as idiomorphic crystals in the ferro-magnesian clots. The alteration products of the biotite and hornblende are always chlorites; secondary epidote frequently accompanies the chlorite in the biotite-hornblende aggregates.

Biotite-granodiorites akin to those of Mount Bransfield also occur at Cape Robinson, on the mainland west of Three Slice Nunatak and in the central core of the peninsula (Knowles, 1945, p. 142). In petrography they resemble the rocks of the Mount Bransfield area, but it is clear that zoning in the plagioclase is more pronounced in the southern granodiorites. This is enhanced by the highly sericitic nature of the plagioclase cores. Another point of some significance is that the biotite in these rocks is almost totally replaced by chlorite.

C. QUARTZ-DIORITES

AS has been remarked by many earlier authors, the quartz-diorites are indeed the commonest of all the igneous intrusive rocks of the Graham Land peninsula. From the northernmost part of Trinity Peninsula south to Cape Adams, on the east coast, and the Eklund Islands, south of Alexander Land, the quartz-diorites occur at almost every locality examined in the field. On both the east and west coasts of the peninsula they form the greater part of the coastline. It is therefore clear that the major part of the batholithic intrusion is composed of quartz-diorite rather than biotite-granite, granodiorite or the more basic diorites and gabbros.

In the majority of localities where the quartz-diorites have been mapped they are characterised by an abundance of zenoliths, most of which are basic in composition (Plate Ic; pages 10–13). However, in the Trinity Peninsula area xenoliths are less common than in the more southerly areas. It is therefore preferable to describe the quartz-diorites individually according to their field occurrences.

1. BLADE RIDGE QUARTZ-DIORITES (HOPE BAY)

The quartz-diorite of Blade Ridge, Hope Bay (Plate Ia), which may be considered as the type diorite of the northern part of Trinity Peninsula, is a medium-grained rock with a hypidiomorphic texture. The plagioclase is usually andesine with a composition ranging from $Ab_{65}An_{35}$ to $Ab_{53}An_{47}$ in the zoned crystals. In the more heavily zoned plagioclases the outermost zones have a composition as acid as $Ab_{75}An_{25}$. The degree of zoning is usually shown up by the marked saussuritisation and sericitisation in the more

calcic zones. Quartz and orthoclase, the latter often considerably altered, are interstitial and play a minor part in the mineralogical composition of the rock. Of the ferro-magnesian minerals, biotite is by far the commonest, forming up to 10% of the mode of the rock. It is of the common type, with pleochroism in straw and deep brown, and is frequently altered marginally to a pale green chlorite. A green hornblende with a pleochroism scheme α = colourless to pale green, β = greenish brown and γ = deep green, accompanies the biotite. The accessory minerals include magnetite, ilmenite (invariably altered to leucoxene marginally), apatite, zircon and sphene. The apatite and zircon often appear as well-defined inclusions in the first generation of biotites, whereas the smaller-sized second generation is free from inclusions.

Epidote, a pale green chlorite with a pleochroism scheme α = pale to colourless, β = pale green and γ = green and showing anomalous interference colours, and actinolite are the secondary alteration products. Chlorite is only associated with the biotite but actinolite and epidote replace hornblende, the former giving rise to narrow rims round the hornblendes.

Xenoliths are rarely found in the Blade Ridge type quartz-diorites except in the immediate vicinity of the contact with the Trinity Peninsula Series. Certainly, basic inclusions are characteristically absent.

2. Marguerite Bay Area

The quartz-diorites of the Marguerite Bay area are petrographically identical to those of Trinity Peninsula. At Red Rock Ridge and the Refuge Islets it is possible to distinguish two separate phases of the quartz-diorite: the first is very fine-grained and the second is coarser, being comparable in texture to the quartz-diorites of Trinity Peninsula. In mineralogy the two phases are similar but field evidence lends little information as to which is the earlier. It can only be assumed that they are contemporaneous. Both of these quartz-diorites intrude the Red Rock Ridge gabbro.

The "quartz-monzonites" described by Knowles (1945) from the Red Rock Ridge area are now included with the fine-grained quartz-diorite phase as they are mineralogically and texturally identical.

3. East Coast of Graham Land

Although the greater part of the east coast of Graham Land south of Three Slice Nunatak is composed of quartz-diorite similar to that of the Marguerite Bay area, there is a further type which occurs in the Cape Bryant area (E.30). This type is mineralogically distinct from the quartz-diorites of the Cape Christmas area (E.29) in that it carries augite in excess of hornblende (E.30.1; Table III). As in the Marguerite Bay area, these diorites also intrude the uralitised gabbros which occur at the same locality. Xenoliths of hornblende-schist, varying widely in shape and size, are frequently included in this quartz-diorite (The Petrology of Graham Land: I. The Basement Complex; Early Palaeozoic Plutonic and Volcanic Rocks).

Unlike the quartz-diorite of Cape Christmas (E.29.1), which is a hornblendic type, the present quartz-diorite has an abundance of augite which is generally altered marginally to an amphibole mineral close to actinolite. The augite, almost colourless and non-pleochroic, is invariably twinned on (101) and occasionally on (100). Its extinction angle, $\gamma : z$, is 46° with a 2V of approximately 60°. The replacing amphibole is readily distinguishable, mainly by its marked pleochroism: α = pale green-brown to colourless, β = green-brown and γ = green-blue. This actinolite has a small extinction angle, $\gamma : z$, of 15° and a 2V of 65°. Replacement by amphibole often occurs around small inclusions in the pyroxene. This amphibole, although retaining the prominent pyroxene (110) cleavage, is different in optical orientation from the original augite.

Plagioclase with a composition approximately $Ab_{60}An_{40}$ forms the greater part of the rock. The andesine is nearly always twinned according to the albite law, and fine repeated zoning is only distinguishable with some degree of difficulty in the larger crystals. Frequent bent twin lamellae indicate that the diorite has undergone a certain amount of strain, probably during cooling. Biotite, which is fairly abundant in the main body of the rock as large well-developed flakes, is often present in the zoned plagioclases as small idiomorphs. The biotite seems to be fairly iron-rich as is indicated by its high refractive index, prominent red colour and pleochroism scheme: $\alpha = \beta$ = pale straw and γ = deep red-brown. Pleochroic haloes are always found surrounding small apatite inclusions. Allotriomorphic interstitial quartz is marginal to the large andesine phenocrysts. Myrmekitic intergrowths are rarely found in these rocks.

A group of rocks which may be included in this section for convenience of description are the hypersthene-bearing quartz-diorites of Trinity Peninsula (D.353.1). Under the microscope they are medium- to fine-grained with a hypidiomorphic granular texture. They are primarily composed of heavily zoned plagioclase, biotite and augite with idiomorphic hypersthene included in the plagioclases. The plagioclase appears clearly as two generations, the first of which exhibits distinct zoning, whereas the second is more acid and unzoned. The composition of the early plagioclases varies from $Ab_{50}An_{50}$ in the cores to $Ab_{64}An_{36}$ at the rims, but the second generation plagioclases are simply twinned and have an overall composition of approximately $Ab_{66}An_{34}$. Ragged augites are often marginally uralitised and the reddish brown biotites are altered to chlorite. The secondary uralite replacing the augite is probably actinolite with pleochroism in pale green and grass green. The idiomorphic hypersthene is frequently twinned but is quite distinctive with its straight extinction and pleochroism scheme α = yellow-pink, β = yellowish brown and γ = pale green. It has a negative 2V of approximately 70°.

Magnetite, apatite and zircon are the accessory minerals. Sometimes calcite occurs as a secondary product in the plagioclases together with sericite and saussurite.

TABLE III

MODAL ANALYSES OF QUARTZ-DIORITES

	E.30.1	1	2	3	4	D.754.1	D.754.4	D.760.3	D.51.1
Quartz	20.1	29.0	11.1	10.0	10.0	17.9	7.3	7.4	16.8
Orthoclase	2.0	2.3	—	40.0	20.0	2.1	—	24.8	—
Andesine	47.0	45.7	57.2	25.0	40.0	60.2	5.7	45.7	66.1
Biotite	18.7	10.4	2.9	5.0	20.0	14.2	10.2	10.9	2.3
Hornblende	1.4	6.3	22.5	15.0	10.0	3.0	51.4	—	10.2
Chlorite	—	*	—	*	*	†	2.3	†	2.2
Magnetite	0.1	6.3	6.3	—	—	0.3	—	0.6	2.1
Augite	10.7	—	—	—	—	—	—	—	—
Sphene	*	—	—	—	—	1.0	*	*	0.1
Apatite	*	—	—	—	—	0.4	*	*	*
Epidote	—	—	—	—	—	1.1	—	10.6	—
Sericite	—	—	—	*	—	—	22.9	—	—

*Indicates present but not estimated.
†Included with biotite.

E.30.1 Quartz-diorite; Cape Bryant.
1 Tonalite; Port Lockroy, Wiencke Island. (Tyrrell, 1921)
2 Quartz-diorite; "Shackleton Harbour",[1] Brabant Island. (Tyrrell, 1921)
3 Quartz-diorite; 5 miles east of Cape Berteaux. (Knowles, 1945)
4 Quartz-diorite; Red Rock Ridge. (Knowles, 1945)
D.754.1 Quartz-diorite; Gulliver Nunatak.
D.754.4 Altered hornblende-biotite-diorite; Gulliver Nunatak.
D.760.3 Granodiorite; Cape Robinson.
D.51.1 Quartz-diorite; Lizard Hill, Tabarin Peninsula.

[1]The bay close northwest of Mount Bulcke, southern Brabant Island.

The modal analyses of some Graham Land quartz-diorites are given in Table III. A close inspection of this table indicates that in the past a large number of rocks have been placed in this category on the basis of the plagioclase composition alone, for example, Nos. 3 and 4 (Table III). Although some of the rocks from the Palmer Archipelago have been described by Tyrrell (1921) as tonalites, their modal composition is nearly that of the quartz-diorites described here. The quartz content of the quartz-diorites is frequently as much as 20%, whereas the orthoclase seldom exceeds 3%. A number of the Hope Bay rocks, which would also be classified here, are described by Bodman (1916) as quartz-mica-diorites.

c. Xenoliths in the Quartz-Diorites

Xenoliths of widely varying composition have been found associated with the quartz-diorite intrusions of the east and west coasts of Graham Land and Trinity Peninsula. In the southern regions of Graham Land the inclusions are predominantly hornblende-schists of a Basement Complex parentage (The Petrology of Graham Land: I. The Basement Complex; Early Palaeozoic Plutonic and Volcanic Rocks, pages 6–9). Local exceptions have been recorded, for instance, in the Terra Firma Islands layered gabbro intrusion, where all the xenoliths incorporated by the gabbro are derived from the nearby Jurassic lavas and tuffs (The Petrology of Graham Land: IV. The Jurassic Volcanics).

In Trinity Peninsula, however, where the Basement Complex has not yet been found *in situ* and where the quartz-diorites frequently invade and often severely contact metamorphose the Trinity Peninsula Series (The Petrology of Graham Land: III. Metamorphic Rocks of the Trinity Peninsula Series), the foreign xenoliths have been plucked from the surrounding country sediments. The grade of metamorphism suffered by the sedimentary inclusions is sometimes very high but complete assimilation is a rarely observed phenomenon.

On both the east and west Graham Land coasts, where hornblende-schists are the commonest xenoliths in the quartz-diorites, contact phenomena show a remarkably close general agreement. In thin section the marginal phase of the quartz-diorite exhibits no marked textural alteration, though there is a tendency towards the interstitial development of delicate quartz-plagioclase symplectic intergrowths. This becomes especially apparent where hornblende and biotite are adjacent. Sometimes quartz forms lenticular segregetions marginal to the contact but seldom to a marked degree. The accessory minerals, zircon and sphene, are present in small amounts.

In the marginal phase of the hornblende-schist xenolith/quartz-diorite contacts there is a distinct increase in the modal quartz and plagioclase from 12 to 21% and 47 to 57% respectively, accompanied by intergranular intergrowths. Hornblende and biotite, on the other hand, show a marked decrease from 21.5 to 16% and 19 to 5% respectively. There is little alteration in the accessory and secondary mineral assemblages, except that sphene decreases and there is the tendency for chlorite to replace biotite.

Quite clearly there has been no pronounced marginal assimilation of hornblende from the hornblende-schist xenoliths by the quartz-diorites. In fact, the contacts are remarkably sharply defined. Plagioclase compositions throughout the quartz-diorite remain at approximately $Ab_{65}An_{35}$, but the total modal ferromagnesians are reduced to almost half the original 41.5% in the zone immediately adjacent the contact.

Although it is true that the presence of xenoliths is a widespread and common feature of the Andean quartz-diorites of Graham Land, the opinion expressed by Barth and Holmsen (1939), that the early Tertiary quartz-diorites are primarily migmatitic or palingenic in origin, completely misrepresents the facts and appears to be founded upon inadequate local evidence and cursory investigations.

D. HORNBLENDE-BIOTITE-DIORITES

DIORITES of this type are subordinate to the quartz-diorites but even so their distribution is more widespread than at first suspected. Their occurrence is well known in the Palmer Archipelago and the Biscoe Islands (Bodman, 1916; Pelikan, 1909; Gourdon, 1908), where they are intruded by the quartz-diorites. However, in the Hope Bay and Marguerite Bay areas they are relatively uncommon. The only hornblende-biotite-diorite of Hope Bay is that referred to as the "Tabarin Peninsula diorite". The Marguerite Bay

occurrence is in the Longridge Head area. Petrographically, the material from both these areas is the same and they may be described together.

In thin section the hornblende-biotite-diorites are medium-grained and possess a hypidiomorphic texture. The main ferro-magnesian minerals are a pale hornblende, with extinction angle, $\gamma:z = 18°$, pleochroism scheme α = pale green, γ = pale bluish-green and $2V = 60°$, and biotite pleochroic in pale straw and deep brown. The plagioclase felspar, which forms the greater part of the rock, is always altered and heavily zoned, ranging in composition from $Ab_{51}An_{49}$ in the core to $Ab_{65}An_{35}$ at the outer rim. Sometimes there is a little interstitial orthoclase and quartz. The accessory minerals include zircon, sphene, titaniferous magnetite and apatite.

Alteration to chlorite is not only confined to the biotite but also occurs in the hornblende. The plagioclase is usually sericitised in the more calcic zones.

Whereas the hornblende-biotite-diorites of the Longridge Head area contain an abundance of basic inclusions, they are relatively unknown in the Tabarin Peninsula diorites.

E. GABBROS

1. Uralitised Hornblende-Gabbros

URALITISED hornblende-gabbros have been recorded in association with and intruded by later quartz-diorites at Cape Bryant (E.30). They are undoubtedly contemporaneous with those of Cape Christmas.

These gabbros are somewhat unusual in view of the fact that among the mafic constituents brown hornblende is frequently in excess of clino-pyroxene. This pale brown hornblende usually contains only minute pyroxene remnants or forms broad rims round the larger irregularly-shaped clino-pyroxenes. Biotite (now altered entirely to chlorite), magnetite, iron pyrites, early plagioclase and apatite all appear as inclusions in the original magmatic hornblende, which is frequently altered to green actinolite both marginally and around the inclusions, especially round the iron ores. The optical properties of this amphibole indicate that it is a common hornblende with pleochroism scheme α = pale straw, β = yellow-brown and γ = dark yellow-brown, extinction angle, $\gamma:z = 17–19°$ and a 2V of approximately 75–80°. Symmetrical twinning on (100) is common.

FIGURE 3

Marginal uralitisation of augite in gabbro; uralite (shaded), augite (with cleavage), magnetite and apatite; Cape Bryant (E.30.4; ordinary light; ×30).

Subsidiary clino-pyroxene (augite or perhaps diallage) is seldom found fresh and unaltered. This pyroxene is colourless in ordinary light, non-pleochroic and usually exhibits simple twinning on (100). The extinction angle, $\gamma : z = 44°$ and the 2V is approximately 60°. It is associated with magmatic brown hornblende and forms well-developed crystals with perfect outline.

Uralitisation both marginally and along cleavage planes is common, actinolite often being the replacing amphibole. Actinolite, with a fibrous structure, also occurs within the rock as a secondary mineral. It has a pleochroism scheme α = pale yellow-green, β = green and γ = bluish green. Its extinction angle is always smaller than that of the brown hornblende, being about 15°. Where iron ore inclusions occur within the clino-pyroxene uralitisation seems to become more intense (Fig. 3).

Basic plagioclase with a composition of $Ab_{40}An_{60}$ forms the greater part of these rocks, except in the case of E.30.4 (Table IV) where brown hornblende and labradorite occur in almost equal porportions. The plagioclase shows albite or combined Carlsbad/albite twinning with rare pericline twinning. Zoning is usually absent but localised saussuritisation is common.

Iron ore, represented largely by magnetite with minor iron pyrites, is widespread throughout the gabbros as large irregular-shaped masses and as inclusions in the brown amphibole. Skeletal magnetite crystals, frequently associated with small felted aggregates of secondary fibrous actinolite, are probably the result of the uralitisation of former clino-pyroxene. Secondary hematite is found as pseudomorphs after iron pyrites.

The accessories include biotite (as inclusions in hornblende and augite, and now altered to chlorite), apatite and sphene. Apart from actinolite, epidote is the only other secondary mineral associated with uralitisation of the clino-pyroxene.

TABLE IV

MODAL ANALYSES OF URALITISED HORNBLENDE-GABBROS

	1	2	3	E.30.5	E.30.4	4
Plagioclase	46.0	44.6	33.0	56.2	39.1	—
Hornblende	25.0	54.3	27.0	11.7	33.7	60.0
Hypersthene	20.0	—	5.0	—	—	—
Enstatite	—	—	—	—	—	10.0
Diallage	—	—	20.0	—	—	—
Diopside	—	—	—	—	—	10.0
Augite	6.0	—	—	8.7	3.5	20.0
Magnetite	2.4	—	10.0	5.3	6.4	—
Hematite	—	—	—	—	0.2	—
Iron pyrites	—	—	—	*	0.3	*
Pyrrhotite	0.6	—	—	—	—	—
Actinolite	—	—	—	13.8	15.9	*
Spinel	—	—	5.0	—	—	—
Apatite	—	—	—	1.0	0.7	—
Epidote	—	—	—	3.2	*	—

*Indicates present but not estimated.

1. Hornblende-norite; Cuyamaca region, California. (Reid, 1902)
2. Uralite-gabbro; Nuljuvaara, Finland. (Hackman, 1905)
3. Hornblende-gabbro; Pavone, Italy. (Van Horn, 1897)

E.30.4 and 5. Uralitised gabbro; Cape Bryant, Graham Land.

4. Hornblendite; "Cape Eielson".[1] (Knowles, 1945)

[1]Now called Eielson Peninsula.

Although E.30.4 and E.30.5 (Table IV) are part of the same gabbro mass, there is a considerable difference in their respective mineralogical compositions. The former is richer in ferro-magnesians, especially brown hornblende, than the latter, but E.30.5 contains more unaltered augite than E.30.4. The plagioclase percentage naturally varies inversely as to the percentage of ferro-magnesians. The only real similarity between these two rocks is that both possess the same amount of iron ore and both have been uralitised to a similar degree. The accessories in each case are identical.

The explanation of this discrepancy in mineralogical composition is that E.30.4 is from one of the more basic layers in the gabbro intrusion, where there has been an accumulation of ferro-magnesians. However, in E.30.5 there is a higher percentage of augite.

The modal analyses of the Cape Bryant uralitised hornblende-gabbros are set out in Table IV, where they are compared with other known gabbros of this type.

From the mineralogical composition and textural relations of these gabbros it is clear that the brown hornblende is of a primary or magmatic origin whereas the green actinolite is secondary, replacing clinopyroxene either totally or in part.

2. Hornblendites

It seems that the hornblendites recorded by Knowles (1945) from Eielson Peninsula are in some way related to the uralitised hornblende-gabbros described above. The hornblendites represent the most basic differentiates of the hornblende-gabbros but they show several phenomena not observed in the latter: they contain no iron ore or plagioclase; the pyroxenes are enstatite, diopside and augite; and there is relatively little uralitisation. The greater part of the hornblende is brown in colour, being characteristically magmatic rather than secondary in origin.

Truly magmatic hornblendites are not very common. It is therefore suggested that in this particular case pyroxene was an early precipitate from the parent magma but was replaced at a late magmatic stage by brown hornblende. This same phenomenon is exhibited by the hornblende-gabbros, in which the brown hornblende contains ragged remnants of pyroxene. Replacement by pale green amphibole is distinctly a secondary process entirely disconnected from the formation of the brown hornblende, which itself is sometimes replaced by actinolite.

The modal composition of the Eielson Peninsula hornblendite is given in Table IV.

3. Gabbros of the Hope Bay Area

Bodman (1916) has described several specimens from the east side of The Pyramid, Nobby Nunatak and Depot Glacier in the Hope Bay area as uralitised olivine-gabbros. The first two localities have been re-examined in some detail and the specimens collected (D.16.1, D.53.1 and D.544.1) agree completely with the material collected and described by Bodman. Nobby Nunatak and the east side of The Pyramid are both part of the same intrusive body but the locality near Depot Glacier is completely disconnected and appears to be a separate intrusion.

These rocks are medium- to coarse-grained in the hand specimen and are greenish-grey in colour. They are characterised by a prominent speckling with a greenish mineral which appears to be a secondary product replacing former phenocrysts in the rock. A number of thin slices from these rocks have been examined under the microscope. They all show a marked hypidiomorphic granular texture and reveal that the rock has suffered considerable alteration. Zoned plagioclase, with a composition of $Ab_{40}An_{60}$ in the cores and $Ab_{56}An_{44}$ at the rims, forms about 50% of the rock. The main ferro-magnesian mineral is a biaxial positive pale augite, which has an extinction angle, $\gamma : z = 37°$ and a $2V = 60°$. Sometimes, where it is in contact with plagioclase, the augite is zoned but this is not common. The augite is invariably uralitised, being mantled with a pale green actinolitic amphibole with an extinction angle, $\gamma : z$, varying between 0° and 10°. Throughout the rock aggregates of serpentine and antigorite occur as pseudomorphs after former olivine phenocrysts. Rarely are the minute cores of the original olivine to be found in the serpentinous felted masses. In addition to uralitisation of the pyroxene there is a reasonably large amount of chlorite in

the matrix. The plagioclases are often altered to either sericite or dusty saussurite. The accessory minerals include magnetite, iron pyrites, ilmenite (altered marginally to leucoxene) and apatite. Iron pyrites may be of a late hydrothermal origin, associated with the later dioritic intrusions in the near vicinity.

The Nobby Nunatak specimens contain no brown magmatic hornblende but the material from the east side of The Pyramid possesses small amounts replacing augite marginally.

At Gulliver Nunatak (D.754) on the King Oscar II Coast similar gabbros to those of the Hope Bay area have been recorded in the granite-gabbro complex, and these are invariably uralitised in the same manner.

4 Gabbros of Marguerite Bay

In this area gabbros are far less usual than elsewhere in Graham Land. So far, only two occurrences north of Neny Fjord and three localities south of Red Rock Ridge have been recorded. At Red Rock Ridge itself a gabbroic mass forms a narrow band traversing the ridge about a quarter of a mile from the westernmost point. From the field relations it is clear that both the Red Rock Ridge granite and the quartz-diorites are younger than the gabbro. In mineralogy this gabbro is similar to the gabbros already described from Hope Bay. The most interesting of all the Marguerite Bay gabbro intrusions is that of the Terra Firma Islands, which will be described at some length later (pages 16–21).

Another occurrence of gabbroic rocks is in the Eklund Islands, south of Alexander Land, where the field relations between them and the other intrusive rocks of Andean affinity are the same as in other localities already mentioned. A small gabbro-like complex, which has only been briefly examined in the field, forms the Buttress Nunataks at the southeast corner of King George VI Sound.

5. Layered Gabbro Intrusion of the Terra Firma Islands

Contrary to the opinion expressed by Nichols (1948), the gabbroic mass which occupies the western part of Alamode Island and all the smaller islets (Barn Rock, Lodge Rock, Hayrick Islet, Twig Rock, Dumbbell Islet and Pigmy Rock) immediately to the north and west of it in the Terra Firma Islands (Fig. 4) is intrusive into the andesitic volcanics. The main evidence for this is the fact that the volcanics are contact metamorphosed by the gabbros. This aspect is examined in detail in a later report (The Petrology of Graham Land: IV. The Jurassic Volcanics) under the heading of "Contact metamorphism of the Terra Firma Volcanics".

This gabbro intrusion is quite extensive; not only does it form a large part of the Terra Firma Islands themselves, but also the Flyspot Rocks and Compass Islet to the north-north-west. The same intrusive body also appears on the mainland to the southeast. The Terra Firma Islands have been mapped (Fig. 4) with particular respect to the gabbro/volcanics contact and the layering within the gabbro itself. In Figs. 5 and 6 the nature of the steep-dipping intrusive contact and the layering in the gabbro are illustrated.

Close to the contact with the volcanics abundant tuffaceous and lava xenoliths occur within the gabbro. All of these have suffered high grade contact metamorphism.

Near the contact two very prominent horizons occur within the gabbro. The lower of these has been called the "Limonite Zone" because of its typical limonitic staining on the weathered surface; the upper malachite-stained horizon has been called the "Malachite Zone". Both these zones are about 20 ft. thick and are separated by about 150 to 200 ft. They follow the contact with marked regularity and have even been recorded on Dumbbell Islet, which is separated from the main group of islands.

Away from the contact the gabbros vary considerably in their mineralogy but at present it is convenient to examine only the nature of the more basic layers and the acid interlayers near the base of the intrusion.

Close to the contact the gabbro is relatively rich in plagioclase, containing approximately 70%. The main ferro-magnesian mineral is augite which is partially replaced marginally by a brown amphibole. Uralitisation of the pyroxene is quite common and a pale actinolite even replaces some of the late magmatic hornblende. The plagioclase is seldom zoned or more acid than in some of the higher layers, having a composition of approximately $Ab_{41}An_{59}$. Pericline twins in the plagioclases are as common as combined albite/Carlsbad twins. The plagioclase is little altered and appears to be relatively fresh. Olivine is notably absent. Among the accessories are apatite, a little biotite and an abundance of iron ore. There is some

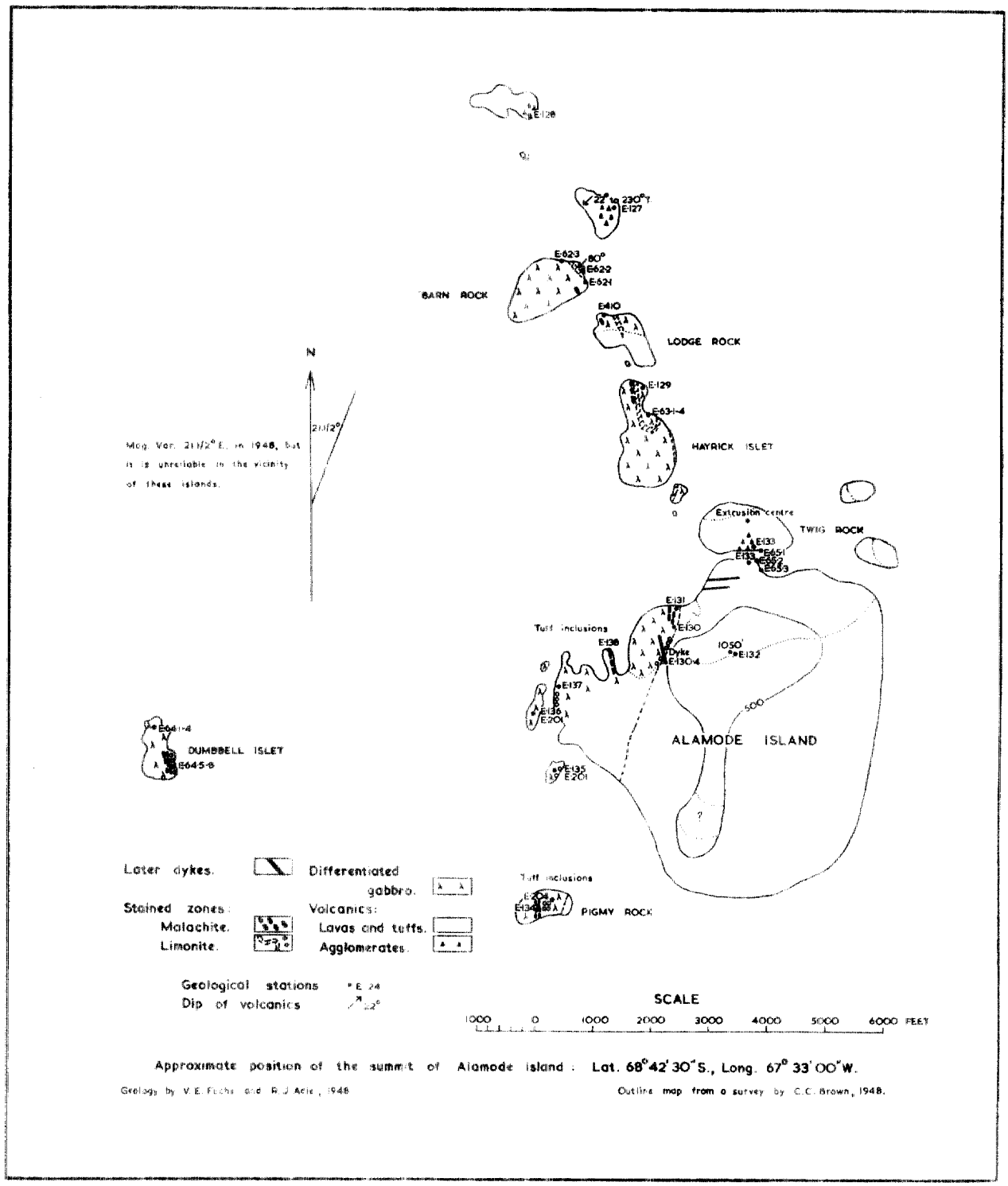

FIGURE 4

Geological sketch map of the Terra Firma Islands, Marguerite Bay, Graham Land (by V. E. Fuchs and R. J. Adie).

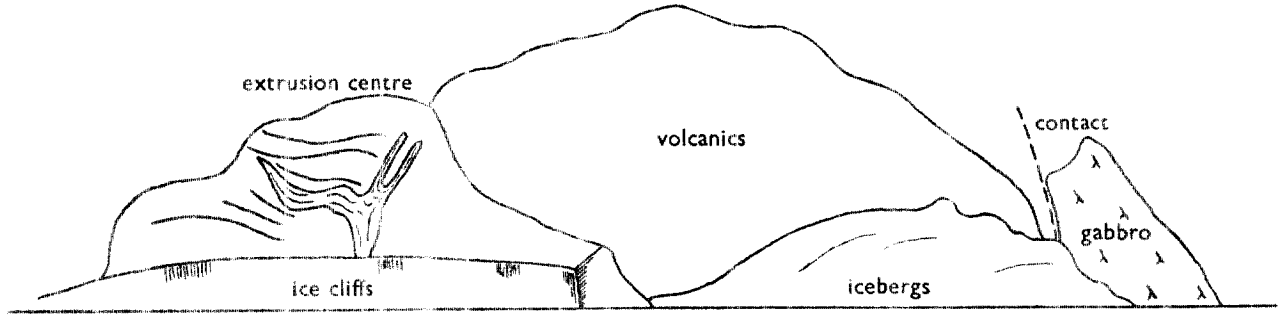

FIGURE 5

A view of Alamode Island, Terra Firma Islands, from the north showing the extrusion centre and the contact between the Jurassic andesitic volcanics and the layered gabbro intrusion (from a drawing by V. E. Fuchs).

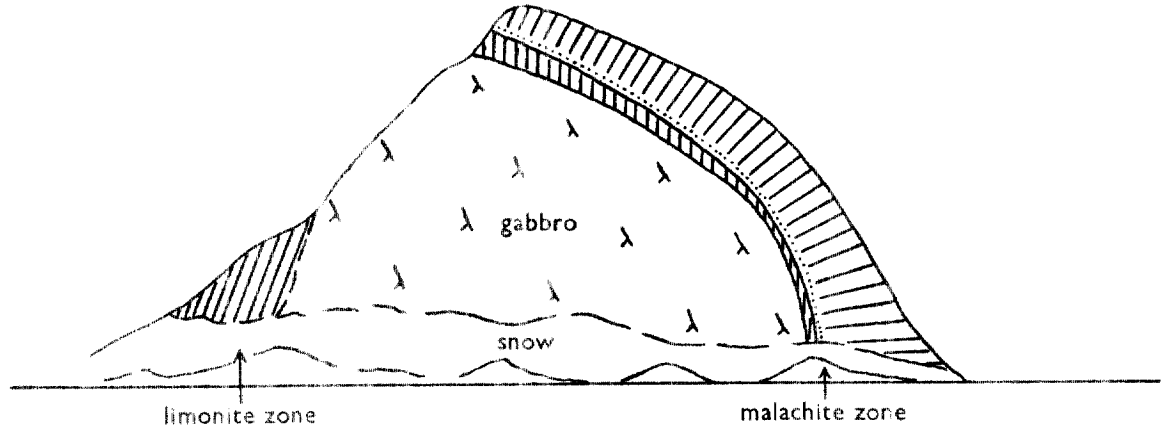

FIGURE 6

Hayrick Islet, Terra Firma Islands, from the north-north-east illustrating layering in the gabbro intrusion and the limonite- and malachite-stained zones (from a drawing by V. E. Fuchs).

secondary chlorite accompanying the uralite. Quartz never occurs in the rocks closest to the contact, but in those about 300 ft. above the base up to 2% is present.

Between the "Limonite and Malachite Zones" the mineralogy of all the rocks is similar, apart from the introduction of a little highly magnesian olivine. The olivine is very fresh in appearance and infrequently altered marginally. It is, however, heavily cracked.

Immediately above the "Malachite Zone" the gabbros become more acid. Quartz may form as much as 12% of the modal composition, olivine disappears completely and the labradorite percentage increases proportionally to the decrease in clino-pyroxene. The overall composition is similar to that of the lower-most gabbros. Iron ore also shows a marked decrease in amount but the other accessory minerals remain fairly constant except in the basic zones themselves.

(i) "Limonite Zone"

The "Limonite Zone" (E.62.2) comprises an assemblage of rocks remarkably rich in iron ore. In thin section the rock is spattered with chunky magnetites and a little hematite. The main ferro-magnesian mineral is augite with schiller structure; it is shrouded in brown magmatic amphibole (hornblende). Uralitisation of the augite is common not only along the crystal boundaries but also along the cleavage planes. Biotite is among the accessories and is generally replaced entirely by chlorite.

In the upper part of the "Limonite Zone", where olivine begins to appear in small amount, it is invariably highly altered to serpentine or a reddish brown mineral (? bowlingite). The plagioclase in this zone is acid bytownite with a composition $Ab_{29}An_{71}$. It shows some degree of alteration but is not especially zoned. Limonite fills all the veins traversing the rock and even enters cleavage planes.

(*ii*) "*Malachite Zone*"

The characteristic features of the "Malachite Zone" are its superficial malachite-staining and its richness in olivine, which forms about 13% of the rock. It is magnesian in composition having a negative $2V = 85°$. In this zone the olivine is idiomorphic and always possesses perfect, pale green, fibrous amphibole reaction rims (Fig. 7) wherever it is in contact with the plagioclase felspar. Though it is difficult to ascertain, it is

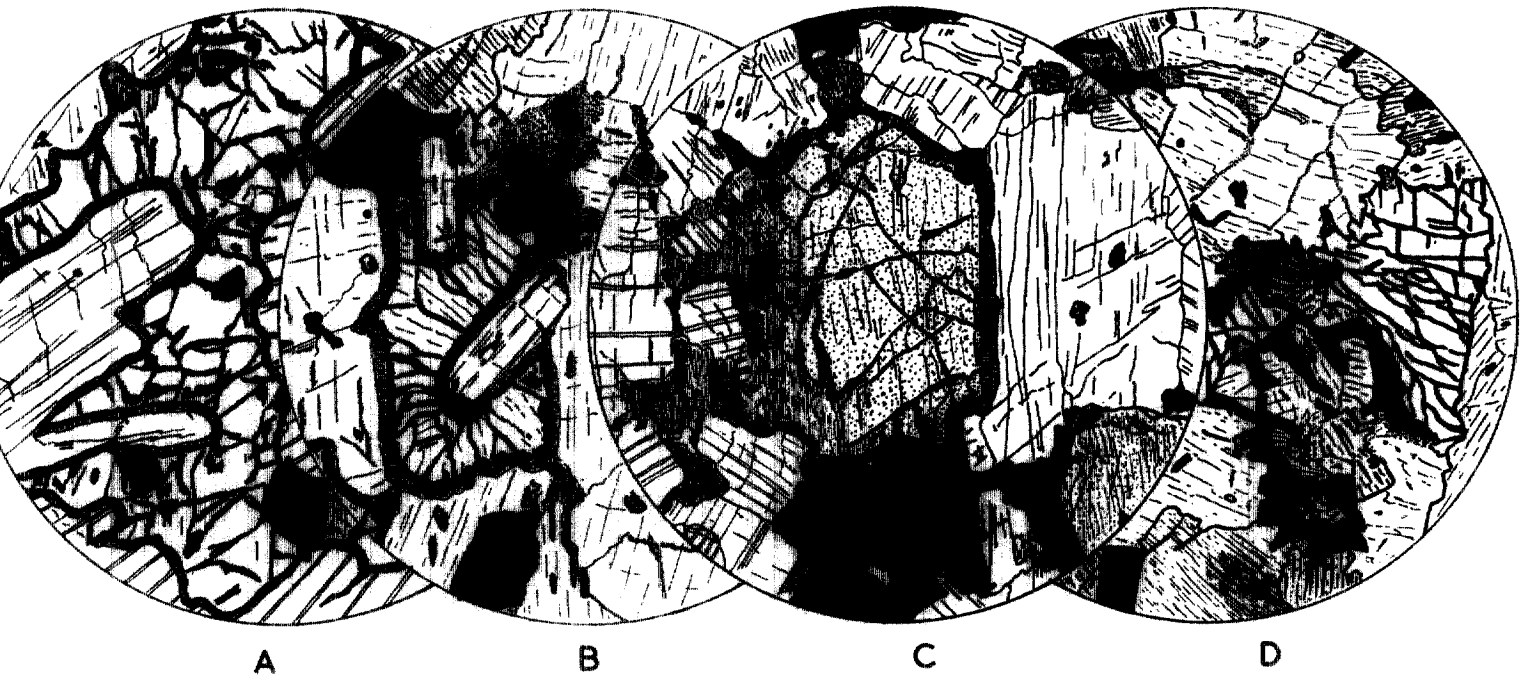

FIGURE 7

Reaction rims round olivines in olivine-gabbros from the Terra Firma layered gabbro intrusion; Terra Firma Islands.

A. Reaction rim of pale green fibrous hornblende round olivines in contact with labradorite. Olivine cracks are filled with (?) bowlingite and iron ore (E.202.1; ordinary light; ×20).

B. The same as fig. 7A but with augite in the upper part of the drawing (E.202.1; ordinary light; ×20).

C. Reaction rim round olivine crystal and replacement by a reddish brown mineral along cracks. Augite in lower part of the drawing (E.64.7; ordinary light; ×20).

D. Heavily cracked olivine partially replaced by serpentine. Iron ore, augite and labradorite are also present (E.64.4; ordinary light; ×20).

considered that these rims are probably a late magmatic feature rather than a distinct secondary one, because serpentinisation and alteration of the olivine have proceeded elsewhere without affecting the amphibole of the reaction rims. The plagioclase with a composition of an intermediate labradorite is fresh and seldom zoned.

Though rhombic pyroxene is an accessory in some of the upper gabbros it does not appear here. Late

magmatic brown amphibole is present in small amount. The iron ores include a relatively high percentage of copper pyrites which gives rise to the malachite staining.

Minor basic layers occur between the two main zones described but they are difficult to trace with any degree of accuracy in the field. Modal analyses of gabbros from the Terra Firma layered intrusion are set out in Table V and the zoning in relation to distance from the contact with the volcanics, based on these modes, is illustrated diagrammatically in Fig. 8.

TABLE V

MODAL ANALYSES OF GABBROS FROM THE TERRA FIRMA ISLANDS

	E.138.1	E.63.3	E.136.1	E.62.1	E.202.1	E.129.2	E.64.7	E.64.2	E.64.4B	E.62.2
Quartz	12.0	2.4	—	2.0	—	0.7	—	—	—	—
Plagioclase	73.3	64.8	64.8	63.2	61.4	56.9	52.4	48.9	38.3	33.6
Clino-pyroxene	—	9.6	19.0	14.5	19.9	26.5	27.6	31.6	29.2	31.0
Rhombic pyroxene	—	1.7	—	0.6	—	1.0	—	—	—	—
Olivine	—	—	—	—	3.3	—	5.1	2.7	12.8	1.7
Magnetite	1.9	6.0	9.2	5.9	8.8	10.6	12.8	13.1	17.2	12.4
Hematite	*	—	—	—	0.3	—	—	—	—	3.9
Cu, Fe pyrites	—	—	0.9	0.3	0.2	—	—	0.2	0.1	0.2
Brown hornblende†	7.9	3.0	0.6	2.1	1.4	0.5	1.1	2.1	1.2	4.4
Green hornblende‡	1.2	9.2	5.5	10.4	4.4	1.8	0.4	1.3	0.4	10.7
Apatite	0.2	—	—	—	—	—	—	—	—	0.1
Biotite	0.6	2.0	—	0.8	—	1.2	—	—	0.1	1.2
Chlorite	2.9	0.3	—	0.2	0.1	0.3	0.6	0.1	0.2	0.6
Serpentine	—	—	—	—	0.2	0.5	—	—	0.5	0.2
Epidote	—	—	—	—	—	—	—	—	0.1	—
TOTAL	100.0	100.0	100.0	100.0	100.0	100.0	100.0	100.0	100.0	100.0
Total Fe Mgs	12.6	25.8	25.1	28.6	29.3	31.8	34.8	37.8	44.5	49.8

*Present, but not in sufficient quantity to be recorded.
†Magmatic amphibole.
‡Secondary amphibole, replacing clino-pyroxene.

E.138.1 Very acid gabbro with quartz
E.63.3 Altered quartz-gabbro
E.136.1 Gabbro
E.62.1 Altered olivine-gabbro
E.202.1 Olivine-gabbro
E.129.2 Gabbro
E.64.7 Olivine-gabbro
E.64.2 Olivine-gabbro
E.64.4B Olivine-gabbro
E.62.2 Altered olivine-gabbro

Although the exact structure of this intrusion is not yet clear, because of the very steep-dipping contact with the volcanics, it is suspected that it may be lopolithic. The segregation of the more basic layers in the marginal part of this intrusion is that of a process of rhythmic banding during the cooling stages. In

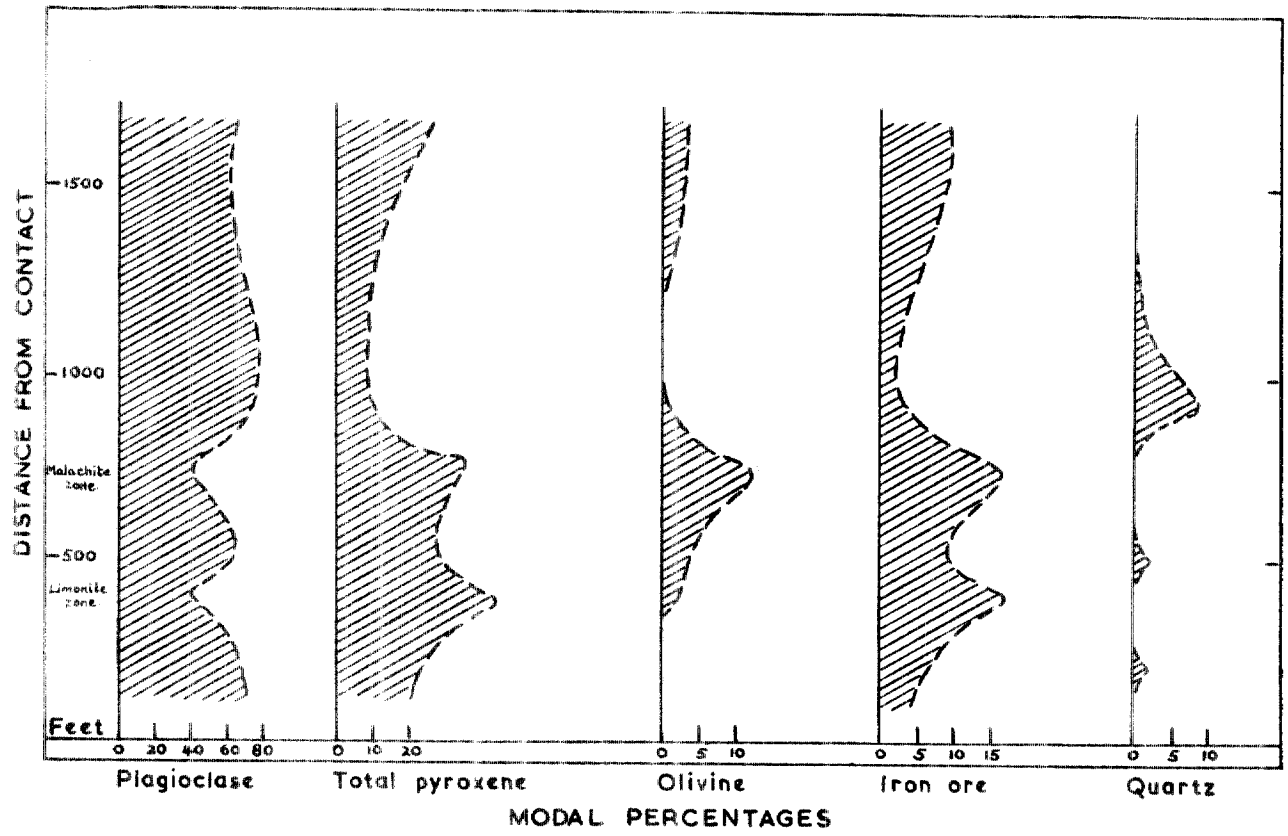

FIGURE 8

The relationship between mineralogical composition and distance from the bottom of the Terra Firma layered gabbro intrusion.

considering the process by which layering took place it must be remembered that the Terra Firma intrusion is small compared with some of the intrusive bodies known from other localities. In this case it seems probable that the gabbro was intruded as one mass, and, though there was probably early fractionation of basic minerals from the magma, local turbulances, aided by convection currents, were responsible for the layering. The parental magma from which the gabbro was derived is not of an olivine-basalt type as has been suggested for the majority of gabbro-norite intrusions, but of a normal calc-alkaline composition. Evidence for this is the relatively acid nature of the rocks near the contact. It is preferable to consider these gabbros as early basic accumulates of the same parental magma from which the later quartz-diorites were also derived.

GEOCHEMISTRY OF THE ANDEAN INTRUSIVE SUITE OF GRAHAM LAND

IN the past the Andean intrusive suite attracted the special attention of several research workers and a considerable amount of time was devoted to the chemical analysis of suitable material from many diverse Graham Land localities and to the statistical interpretation of the data thus obtained. Gourdon (1908), Pelikan (1909) and Bodman (1916) have contributed thirty-three chemical analyses, which are set out in Table VI. In Fig. 9 these earlier analyses are recalculated on a water-free basis and plotted on triangular variation diagrams with the co-ordinates $(FeO+Fe_2O_3)$ – – Alk – – MgO and K_2O – – Na_2O – – CaO. It is, however, unfortunate that no trace element data are available for these rocks.

TABLE VI. PREVIOUS CHEMICAL ANA

	1	2	3	4	5	6	7	8	9	10	11	12	13	14	15	
SiO_2	36.76	43.29	45.84	46.67	47.51	48.11	48.50	48.57	49.68	49.69	50.54	50.66	50.98	51.16	51.56	5
TiO_2	3.85	1.14	0.18	0.48	0.48	0.33	1.32	1.07	0.28	0.99	0.89	—	1.25	0.07	1.34	
Al_2O_3	11.00	21.11	20.42	17.08	23.03	23.08	19.26	19.00	9.84	20.07	17.30	19.70	17.60	16.12	17.95	1
Fe_2O_3	14.21	4.98	6.51	—	1.08	2.29	4.24	—	—	2.47	—	—	—	7.09	3.46	
FeO	12.24	3.50	6.68	8.87*	4.06	3.28	5.26	8.16*	16.00*	5.22	7.91*	9.48*	10.21*	7.24	6.93	
MnO	—	—	tr	—	—	—	—	—	—	—	—	—	—	0.15	—	
MgO	7.55	6.48	4.85	9.57	6.69	5.55	4.63	4.99	8.12	5.75	3.18	5.03	4.61	3.68	5.54	
CaO	11.90	13.25	13.27	11.59	15.08	14.53	12.86	9.80	9.83	12.20	9.62	10.23	9.88	8.55	7.05	
Na_2O	0.95	1.34	1.13	3.28	1.41	1.81	2.02	1.80	3.49	2.39	3.93	4.19	1.21	3.33	3.56	
K_2O	0.22	0.26	0.23	0.69	0.22	0.23	1.06	2.70	0.67	0.45	3.53	1.16	1.93	0.57	1.28	
H_2O+	1.36	0.12	1.27	0.71	0.98	0.88	0.50	0.62	0.55	0.54	1.20	0.71	0.98	1.52	1.58	
H_2O-	—					—	—	—	—	—	—	—	—	—	—	
CO_2	—	—	—	—	—	—	—	—	—	—	—	—	—	—	—	
P_2O_5	—	tr	0.04		—	0.06	0.19	—	—	0.09			—	0.96	0.10	
S	—	—	—	—	—	—	—	—	—	—	—	—	—	—	—	
TOTAL	99.98	100.52	100.38	98.94	100.38	100.15	99.84	96.71	98.46	99.76	98.10	101.16	98.65	100.44	100.35	

* Fe_2O_3 and FeO determined as FeO

1. Gabbro, Cape Tuxen. (Gourdon, 1908)
2. Gabbro, Petermann Island. (Gourdon, 1908)
3. Gabbro, "Bob Island".[1] (Pelikan, 1909)
4. Uralitised olivine-gabbro, Hope Bay. (Bodman, 1916)
5. Gabbro, Léonie Islands. (Gourdon, 1908)
6. Gabbro, Webb Island. (Gourdon, 1908)
7. Gabbro, Jenny Island. (Gourdon, 1908)
8. Hornblende-gabbro, Hope Bay. (Bodman, 1916)
9. Uralitised olivine-gabbro, Hope Bay. (Bodman, 1916)
10. Gabbro, dredged block. (Gourdon, 1908)
11. Augite-diorite, erratic from Snow Hill Island. (Bodman, 1916)
12. Olivine-gabbro, Hope Bay. (Bodman, 1916)
13. Titanite-diorite, Hope Bay. (Bodman, 1916)
14. Augite-diorite, Moreno Island. (Pelikan, 1909)
15. Gabbro, Jenny Island. (Gourdon, 1908)
16. Gabbro, Anvers Island. (Pelikan, 1909)
17. Quartz-diorite, "Cape Anna Osterrieth".[2] (Pelikan, 1909)

[1] Now The island south of Fridtjof Island.
[2] Now Cape Anna.

EAN INTRUSIVE SUITE OF GRAHAM LAND

9	20	21	22	23	24	25	26	27	28	29	30	31	32	33	
.30	57.46	57.98	58.35	58.85	58.97	59.85	61.79	63.01	64.33	64.67	66.39	67.59	71.10	73.26	SiO_2
.06	1.15	0.84	0.80	0.82	1.64	0.84	1.22	0.56	n.d.	0.51	0.33	0.28	0.46	tr	TiO_2
.91	15.95	18.18	16.91	17.48	16.75	16.90	16.20	13.61	16.71	15.39	17.62	14.63	14.50	12.60	Al_2O_3
.15	1.96	2.00	1.79	2.98	—	1.92	2.64	—	—	—	1.01	—	0.31	0.34	Fe_2O_3
.38	5.83	4.59	5.71	3.27	7.96*	5.22	3.62	6.35*	4.52*	5.26*	2.21	5.55*	3.10	2.65	FeO
r	—	—	—	—	—	—	—	—	—	—	—	—	—	—	MnO
.64	3.73	3.67	4.34	2.53	2.06	3.12	1.96	2.42	1.60	1.41	1.32	1.34	1.17	0.51	MgO
.10	7.25	7.28	6.88	6.24	5.67	6.63	4.68	4.29	4.47	3.89	3.79	3.46	2.59	tr	CaO
.43	2.25	1.26	2.99	3.56	4.38	3.45	3.69	2.15	4.36	1.98	4.49	3.34	3.25	5.37	Na_2O
.17	2.82	4.07	1.33	1.97	1.71	1.28	2.98	5.56	2.91	4.61	2.13	3.64	4.02	3.95	K_2O
.74	1.60	0.45	0.33	2.03	0.91	0.87	0.78	0.57	0.34	0.29	0.39	0.91	0.25	0.75	H_2O+
—	—	—	—	—	—	—	—	—	—	—	—	—	—	—	H_2O-
—	—	—	—	—	—	—	—	—	—	—	—	—	—	—	CO_2
.16	0.13	0.12	—	0.12	0.38	0.06	0.28	—	—	—	—	—	0.03	—	P_2O_5
—	—	—	—	—	—	—	—	—	—	—	—	—	—	—	S
.02	99.76	100.44	99.45	99.85	100.65	100.08	99.84	98.55	99.24	98.01	99.68	100.74	100.75	99.42	TOTAL

* Fe_2O_3 and FeO determined as FeO.

18. Quartz-diorite, Moreno Island. (Pelikan, 1909)
19. Quartz-diorite, Two Hummock Island. (Pelikan, 1909)
20. Quartz-diorite, Hovgaard Island. (Gourdon, 1908)
21. Quartz-mica-diorite, "Wandel Island".[3] (Gourdon, 1908)
22. Quartz-biotite-diorite, Hovgaard Island. (Gourdon, 1908)
23. Quartz-diorite, "Berthelot Islands".[4] (Gourdon, 1908)
24. Quartz-diorite, erratic from "Cape Hamilton". (Bodman, 1916)
25. Quartz-diorite, "Wandel Island".[3] (Gourdon, 1908)
26. Diorite, dredged block. (Gourdon, 1908)
27. Quartz-mica-diorite, erratic from Hope Bay. (Bodman, 1916)
28. Quartz-mica-diorite, erratic from Hope Bay. (Bodman, 1916)
29. Quartz-mica-diorite, Hope Bay. (Bodman, 1916)
30. Quartz-diorite, dredged block. (Gourdon, 1908)
31. Tonalite, erratic from "Cape Borchgrevink".[5] (Bodman, 1916)
32. Granite, "Wandel Island".[3] (Gourdon, 1908)
33. Micro-granite, "Wandel Island".[3] (Gourdon, 1908)

[3] Now Booth Island.
[4] Now Berthelot Islets.
[5] Now Borchgrevink Nunatak.

In the course of the present work twelve new representative chemical analyses of the early Tertiary Andean intrusive series of Graham Land have been completed. They include two analyses of olivine-gabbros from the Terra Firma Islands layered intrusion (Tables VIIa, b and c, Nos. 1 and 2), which are interpreted as basic accumulates. The other ten analyses include representatives of the biotite- and amphibole-diorites, the ubiquitous quartz-diorites and the granites (Tables VIIa, b and c, Nos. 3 to 12). The chemical analyses (complete and recalculated on a water-free basis), major and trace elements (in p.p.m.), norms and other relevant data are given in Tables VIIa, b and c. These data are interpreted graphically in two ways:

(1) As triangular variation diagrams with co-ordinates (Fe′′′+Fe′′)—Alk—Mg and K—Na—Ca in Fig. 10. The present results are compared with earlier analyses (Table VI) on similar diagrams with the co-ordinates ($FeO+Fe_2O_3$)—Alk—MgO and K_2O—Na_2O—CaO in Fig. 9.

TABLE VIIa

NEW CHEMICAL ANALYSES OF THE ANDEAN GRANITE-GABBRO INTRUSIVE SUITE OF GRAHAM LAND

	1	2	3	4	5	6	7	8	9	10	11	12	
SiO_2	40.19	50.68	52.83	54.73	59.67	59.94	60.36	60.80	61.03	61.45	69.00	73.44	SiO_2
TiO_2	1.74	1.40	0.90	0.81	0.72	0.58	0.92	0.65	0.65	0.80	0.22	0.22	TiO_2
Al_2O_3	15.53	20.47	19.38	19.38	16.99	18.12	17.01	16.08	15.87	16.58	16.93	14.33	Al_2O_3
Fe_2O_3	8.88	2.84	2.87	0.47	2.77	3.19	1.43	2.35	2.26	2.83	0.63	0.52	Fe_2O_3
FeO	8.99	6.06	4.88	7.63	4.04	2.63	3.93	3.00	3.22	2.87	1.65	1.18	FeO
MnO	0.17	0.14	0.12	0.13	0.10	0.08	0.07	0.09	0.08	0.10	0.04	0.02	MnO
MgO	8.04	3.84	4.34	3.74	2.55	2.00	2.64	3.50	2.94	2.37	0.60	0.21	MgO
CaO	13.96	9.93	9.31	8.28	5.89	6.60	4.14	5.31	5.71	5.70	3.68	2.13	CaO
Na_2O	1.17	3.11	3.19	2.52	3.48	2.88	3.47	3.97	3.56	3.36	3.16	3.09	Na_2O
K_2O	0.03	0.53	1.72	1.91	2.61	2.27	2.95	2.09	2.52	2.78	3.29	3.87	K_2O
H_2O+	0.69	0.51	0.45	0.65	0.49	0.81	2.34	1.55	1.57	0.67	0.76	0.52	H_2O+
H_2O-	0.10	0.08	0.07	0.10	0.16	0.10	0.11	0.12	0.21	0.11	0.11	0.11	H_2O-
P_2O_5	0.36	0.45	0.27	0.56	0.35	0.34	0.41	0.33	0.19	0.36	0.11	0.29	P_2O_5
CO_2	—	—	tr	—	tr	0.29	0.06	0.09	—	—	—	—	CO_2
TOTAL	100.05	100.12	100.33	99.91	99.82	99.83	99.84	99.93	99.81	99.98	100.18	99.93	TOTAL
ANALYSES LESS TOTAL WATER (Recalculated to 100)													
SiO_2	40.49	50.96	52.93	54.19	60.17	60.59	61.98	61.88	62.26	61.95	69.48	73.96	SiO_2
TiO_2	1.95	1.41	0.90	0.82	0.73	0.59	0.94	0.66	0.66	0.81	0.22	0.22	TiO_2
Al_2O_3	15.65	20.58	19.42	19.54	17.13	18.32	17.47	16.36	16.19	16.71	17.05	14.43	Al_2O_3
Fe_2O_3	8.95	2.86	2.88	0.47	2.79	3.22	1.47	2.39	2.31	2.85	0.63	0.52	Fe_2O_3
FeO	9.06	6.09	4.89	7.69	4.07	2.66	4.04	3.05	3.28	2.89	1.66	1.19	FeO
MnO	0.17	0.14	0.12	0.13	0.10	0.08	0.07	0.09	0.08	0.10	0.04	0.02	MnO
MgO	8.10	3.86	4.35	3.77	2.57	2.02	2.71	3.56	3.00	2.39	0.60	0.21	MgO
CaO	14.06	9.98	9.33	8.35	5.94	6.67	4.25	5.40	5.82	5.75	3.71	2.15	CaO
Na_2O	1.18	3.13	3.20	2.54	3.51	2.91	3.56	4.04	3.63	3.39	3.18	3.11	Na_2O
K_2O	0.03	0.53	1.73	1.93	2.63	2.29	3.03	2.13	2.57	2.80	3.31	3.90	K_2O
P_2O_5	0.36	0.45	0.27	0.56	0.35	0.34	0.42	0.34	0.19	0.36	0.11	0.29	P_2O_5
CO_2	—	—	tr	—	tr	0.29	0.06	0.09	—	—	—	—	CO_2
NORMS													
Q	—	3.60	4.98	5.04	13.14	17.88	15.00	13.56	14.64	16.38	27.90	36.00	Q
or	—	2.78	10.01	11.12	15.57	13.34	17.79	12.23	15.01	16.68	19.46	22.80	or
ab	9.96	26.20	27.25	20.96	29.34	24.63	29.34	34.06	29.87	28.82	27.25	26.20	ab
an	36.97	40.59	35.36	36.14	23.07	29.47	17.79	19.74	20.02	21.68	18.35	8.62	an
di	23.54	4.08	8.74	1.14	2.72	1.11	—	3.77	6.67	3.09	—	—	di
hy	1.36	14.08	12.83	21.01	9.03	1.52	11.09	9.38	6.98	6.02	3.61	1.95	hy
ol	9.93	—	—	—	—	—	—	—	—	—	—	—	ol
mt	12.99	4.18	4.18	0.70	4.18	4.64	2.09	3.48	3.25	4.18	0.93	0.70	mt
il	3.65	3.74	1.67	1.52	1.37	1.22	1.67	1.37	1.37	1.52	0.46	0.46	il
he	—	—	—	—	—	—	—	—	—	—	—	—	he
ap	1.01	1.34	0.67	1.34	1.01	0.67	1.01	0.67	—	1.01	—	0.67	ap
C	—	—	—	—	—	—	1.53	—	—	—	1.33	1.84	C
Plag. comp.	$Ab_{24}An_{76}$	$Ab_{39}An_{61}$	$Ab_{45}An_{55}$	$Ab_{39}An_{61}$	$Ab_{56}An_{44}$	$Ab_{46}An_{54}$	$Ab_{62}An_{38}$	$Ab_{63}An_{37}$	$Ab_{60}An_{40}$	$Ab_{57}An_{43}$	$Ab_{60}An_{40}$	$Ab_{75}An_{25}$	Plag. comp.
S.G.	3.19	2.89	2.83	2.84	2.77	2.72	2.69	2.72	2.72	2.69	2.66	2.61	S.G.

(2) As linear variation diagrams with the recalculated element percentages plotted against the function [(1/3Si+K)-(Ca+Mg)] in Figs. 11, 12, 13 and 14.

For convenience of comparison, the new analytical data for major and trace elements and relevant ratios in Tables VIIa, b and c have been set out in the same way as those given by Nockolds and Allen (1953) in their comprehensive study of some calc-alkali igneous rock series. For the same reason, all the variation diagrams (Figs. 10 to 15) based on these new data have been reduced to exactly the same scale as those given by Nockolds and Allen (1953).

When plotted on both (Fe″+Fe‴)--Alk--Mg and K--Na--Ca triangular variation diagrams, one of the analyses (Table VII, No. 8; Fig. 10) departs quite considerably from the smooth curves on which the other rocks lie. A microscopic examination of thin slices of this particular rock reveals that it has been extensively altered. Nevertheless, it is a legitimate member of this series.

TABLE VIIb

NEW CHEMICAL ANALYSES OF THE ANDEAN GRANITE-GABBRO INTRUSIVE SUITE OF GRAHAM LAND

	1	2	3	4	5	6	7	8	9	10	11	12	Sensitivity in p.p.m.	Ionic radius	
Si^{+4}	189.10³	238.10³	247.10³	253.10³	281.10³	283.10³	289.10³	289.10³	291.10³	289.10³	324.10³	345.10³	—	0.42	Si^{+4}
Al^{+3}	83.10³	109.10³	103.10³	103.10³	91.10³	97.10³	93.10³	87.10³	86.10³	88.10³	90.10³	76.10³	—	0.51	Al^{+3}
Fe^{+3}	63.10³	20.10³	20.10³	4.10³	20.10³	22.10³	11.10³	17.10³	16.10³	20.10³	4.10³	4.10³	—	0.64	Fe^{+3}
Mg^{+2}	49.10³	23.10³	26.10³	23.10³	16.10³	12.10³	16.10³	22.10³	18.10³	14.10³	4.10³	1.10³	—	0.66	Mg^{+2}
Fe^{+2}	71.10³	47.10³	38.10³	60.10³	32.10³	21.10³	31.10³	24.10³	26.10³	22.10³	13.10³	9.10³	—	0.74	Fe^{+2}
Na^{+1}	9.10³	23.10³	24.10³	19.10³	26.10³	22.10³	27.10³	30.10³	27.10³	25.10³	24.10³	23.10³	—	0.97	Na^{+1}
Ca^{+2}	101.10³	71.10³	66.10³	60.10³	42.10³	48.10³	31.10³	39.10³	41.10³	41.10³	26.10³	16.10³	—	0.99	Ca^{+2}
K^{+1}	tr	4.10³	14.10³	16.10³	22.10³	19.10³	25.10³	17.10³	22.10³	23.10³	27.10³	32.10³	—	1.33	K^{+1}
Ti^{+4}	117.10²	85.10²	54.10²	49.10²	44.10²	35.10²	56.10²	40.10²	40.10²	49.10²	13.10²	13.10²	—	0.68	Ti^{+4}
Mn^{+2}	13.10²	11.10²	9.10²	10.10²	8.10²	6.10²	5.10²	7.10²	6.10²	8.10²	3.10²	2.10²	—	0.80	Mn^{+2}
P^{+5}	16.10²	20.10²	12.10²	25.10²	15.10²	15.10²	18.10²	15.10²	8.10²	16.10²	5.10²	13.10²	—	0.35	P^{+5}
O^{-2}	420.10³	453.10³	455.10³	454.10³	463.10³	470.10³	469.10³	469.10³	468.10³	471.10³	486.10³	491.10³	—	1.32	O^{-2}
Be^{+2}	*	*	*	*	*	*	*	*	*	*	*	*	5	0.35	Be^{+2}
Ga^{+3}	25	30	20	30	22	20	25	25	20	25	20	15	2	0.62	Ga^{+3}
Cr^{+3}	20	45	tr	8	5	*	25	100	40	10	10	*	2	0.63	Cr^{+3}
V^{+3}	800	300	225	150	150	100	100	300	100	125	30	*	5	0.74	V^{+3}
Mo^{+4}	*	*	*	*	*	15	*	*	*	*	*	*	2	0.70	Mo^{+4}
Li^{+1}	2	6	15	15	20	30	50	25	20	10	35	8	1	0.68	Li^{+1}
Ni^{+2}	80	20	5	15	3	*	15	15	15	*	*	*	3	0.69	Ni^{+2}
Co^{+2}	80	35	25	25	25	10	10	10	10	10	*	*	3	0.72	Co^{+2}
Sc^{+3}	50	20	30	*	*	*	*	*	*	*	*	*	10	0.81	Sc^{+3}
Zr^{+4}	30	80	60	125	200	100	100	150	125	100	60	*	10	0.79	Zr^{+4}
Y^{+3}	*	15	25	25	30	20	20	20	25	25	15	*	10	0.92	Y^{+3}
La^{+3}	*	*	*	*	*	*	*	*	*	*	*	*	40	1.14	La^{+3}
Sr^{+2}	1000	1500	300	1000	1000	900	1500	600	800	750	500	200	2	1.12	Sr^{+2}
Pb^{+2}	*	*	*	*	*	*	55	20	20	*	30	20	10	1.20	Pb^{+2}
Ba^{+2}	50	400	400	650	1000	1500	500	1000	800	1000	1000	650	5	1.34	Ba^{+2}
Rb^{+1}	*	10	70	125	100	150	70	450	150	200	125	200	10	1.47	Rb^{+1}
Cs^{+1}	*	*	*	*	*	*	*	*	*	*	*	*	15	1.67	Cs^{+1}
Tl^{+1}	*	*	*	*	*	*	*	*	*	*	*	*	2	1.47	Tl^{+1}
Position [(⅓Si+K)-(Ca+Mg)]	−8.7	−3.1	+0.4	+1.7	+5.8	−5.2	−7.4	−5.2	+6.0	−6.4	+10.5	+13.0			Position [(⅓ Si+K)-(Ca+Mg)]
Fe	73	74	69	74	76	78	72	65	70	75	81	93			Fe
Mg	27	26	31	26	24	22	28	35	30	25	19	7			Mg
Fe	69	57	48	52	43	45	38	37	39	40	24	19			Fe
Mg	26	20	21	19	14	12	15	20	17	13	6	1			Mg
Alk	5	23	31	29	41	43	47	43	44	47	70	80			Alk
Ca	92	73	64	63	47	54	37	45	46	46	34	23			Ca
Na	8	23	23	20	29	25	33	35	30	28	31	32			Na
K	tr	4	13	17	24	21	30	20	24	26	35	45			K

* Indicates below degree of sensitivity
All values for elements in this table are given in p.p.m.

TABLE VIIc

NEW CHEMICAL ANALYSES OF THE ANDEAN GRANITE-GABBRO INTRUSIVE SUITE OF GRAHAM LAND

	1	2	3	4	5	6	7	8	9	10	11	12	
Ga×1000/Al	0.30	0.28	0.19	0.29	0.24	0.21	0.27	0.29	0.23	0.28	0.22	0.20	Ga×1000/Al
Cr×1000/Mg	0.41	0.96	*	0.35	0.31	*	1.56	4.55	2.22	0.71	2.50	*	Cr×1000/Mg
V×1000/Mg	16.33	13.04	8.65	6.52	9.38	8.33	6.25	4.55	5.56	8.93	7.50	*	V×1000/Mg
Li×1000/Mg	0.04	0.26	0.58	0.65	1.25	2.50	3.13	1.14	1.11	0.71	8.75	8.00	Li×1000/Mg
Ni×1000/Mg	1.63	0.87	0.19	0.65	0.19	*	0.94	0.68	0.83	*	*	*	Ni×1000/Mg
Co×1000/Mg	1.63	1.52	0.96	1.09	1.56	0.83	0.63	0.45	0.56	0.71	*	*	Co×1000/Mg
Fe/Mg	2.73	3.91	2.23	2.78	3.28	3.58	2.63	1.86	2.33	3.00	4.25	13.00	Fe/Mg
Sc×1000/Mg	1.02	0.87	1.15	*	*	*	*	*	*	*	*	*	Sc×1000/Mg
Cr×1000/Fe	0.15	0.67	*	0.13	0.10	*	0.60	2.44	0.95	0.24	0.59	*	Cr×1000/Fe
V×1000/Fe	5.97	4.48	3.88	2.34	2.88	2.33	2.38	2.44	2.38	2.98	1.76	*	V×1000/Fe
Co×1000/Fe	0.60	0.52	0.43	0.39	0.48	0.23	0.24	0.24	0.24	0.24	*	*	Co×1000/Fe
Sc×1000/Fe	0.37	0.30	0.52	*	*	*	*	*	*	*	*	*	Sc×1000/Fe
Y×1000/Ca	*	0.21	0.38	0.42	0.71	0.42	0.65	0.51	0.61	0.61	0.58	*	Y×1000/Ca
Sr×100/Ca	0.99	2.11	0.45	1.67	2.33	1.88	4.84	1.54	1.95	1.83	1.92	1.25	Sr×100/Ca
Sr×100/Ca+K	0.99	2.00	0.38	1.32	1.56	1.34	2.68	1.07	1.27	1.17	0.94	0.42	Sr×100/Ca+K
Ba×100/K	*	10.00	2.86	4.06	4.55	7.89	2.00	5.88	3.64	4.35	3.70	2.03	Ba×100/K
Rb×100/K	*	0.25	0.50	0.78	0.45	0.79	0.28	2.65	0.68	0.87	0.46	0.63	Rb×100/K

EXPLANATION OF TABLES VIIa, b and c

1. E.64.2 Olivine-gabbro, Terra Firma Islands, Marguerite Bay. (anal. R. J. Adie)
2. E.63.3 Quartz-gabbro, Terra Firma Islands, Marguerite Bay. (anal. R. J. Adie)
3. D.76.4 Quartz-gabbro, Last Hill, Trinity Peninsula. (anal. R. J. Adie)
4. E.30.1 Quartz-biotite-diorite, Cape Bryant, Black Coast. (anal. R. J. Adie)
5. D.353.1 Hypersthene-bearing quartz-diorite, Mount Bransfield area, Trinity Peninsula. (anal. R. J. Adie)
6. D.47.1 Quartz-biotite-diorite, Mineral Hill, Trinity Peninsula. (anal. R. J. Adie)
7. D.754.1 Quartz-biotite-diorite, Gulliver Nunatak, King Oscar II Coast. (anal. R. J. Adie)
8. E.114.1 Quartz-diorite, Millerand Island, Marguerite Bay. (anal. R. J. Adie)
9. E.116.1 Quartz-diorite, Millerand Island, Marguerite Bay. (anal. R. J. Adie)
10. D.33.1 Quartz-diorite, Brown Bluff, Tabarin Peninsula. (anal. R. J. Adie)
11. D.375.2 Biotite-granite, Mount Reece, Trinity Peninsula. (anal. R. J. Adie)
12. D.337.1 Biotite-granite, Cape Roquemaurel, Trinity Peninsula. (anal. R. J. Adie)

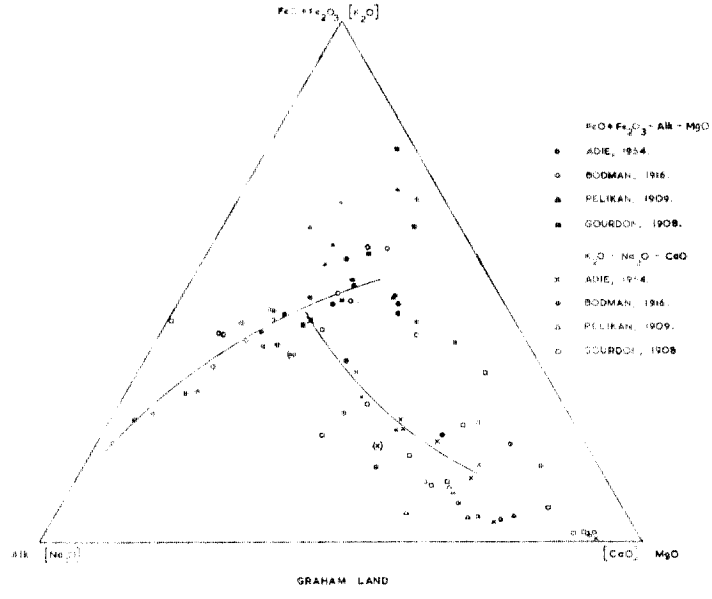

FIGURE 9

Variation diagrams $(FeO+Fe_2O_3)$ – Alk – MgO and K_2O – Na_2O – CaO based on previous and new analyses of Andean intrusives from Graham Land.

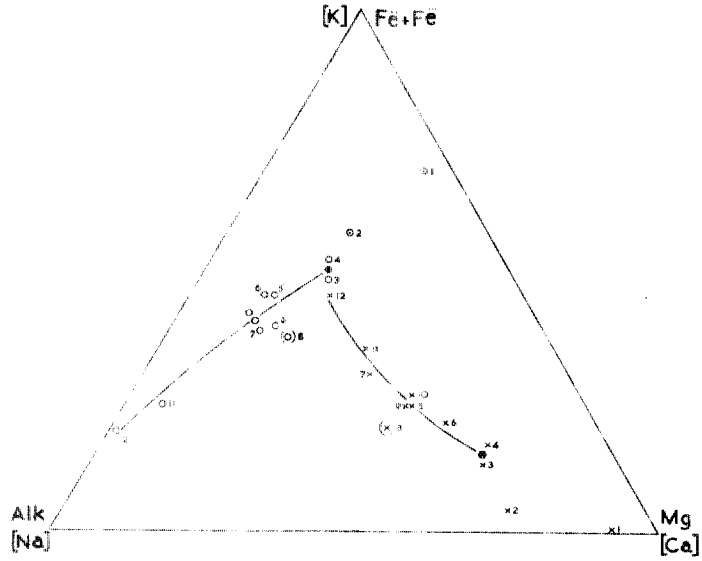

FIGURE 10

Variation diagrams (Fe″+Fe‴) – Alk (K+Na) – Mg and K – Na – Ca based on the new analyses of Andean intrusives from Graham Land. The approximate positions of the parental magma are indicated by (●) and (⊗) respectively. The rock shown in brackets has been altered.

1. Distribution of the Major Elements

The distribution of the major elements of this series is given in Tables VIIa and b. In Figs. 11, 12 and 13 the weight percentages of the elements are plotted vertically against the function [(1/3Si+K)—(Ca+Mg)] so that their distribution may be compared directly with that of the trace elements. In the past it has been the practice to plot oxides, rather than elements which is the method used here. The function against which the elements are plotted in the present linear variation diagrams is comparable to that employed in the Larsen variation diagram, [(1/3SiO_2+K_2O)—(CaO+MgO+FeO)], except that Fe is not included with (Ca+Mg). It is, therefore, possible to detect iron enrichment in a particular series and to use the same function whether the series to be plotted has a calc-alkali, alkali or tholeiitic affinity.

Silicon and Oxygen (Table VIIb; Fig. 11). The actual values for both silicon and oxygen show a regular increase with increasing acidity and both curves follow approximately the same slope over the range examined.

Aluminium, Magnesium, Iron and Calcium (Table VIIb; Figs. 11, 12 and 13). As would be expected, all these elements have a high concentration in the basic rocks and there is a linear decrease in amount towards the acid end of the series.

Sodium and Potassium (Table VIIb; Fig. 13). Potassium follows an increasing trend in amount towards the acid rocks, but there is a greater concentration of sodium in the diorite range than in either the basic or acid members. Accordingly, the K/Na ratio increases markedly with increasing acidity.

2. Distribution of the Trace Elements

The concentrations of the trace elements in parts per million are given in Table VIIb and are illustrated in Figs. 11, 12, 13 and 14, where they are plotted against the function [(1/3Si+K)—(Ca+Mg)] and may be compared directly with the trends of the major elements (in weight percentages) plotted against the same function. Some of the relationships between certain trace and major elements are given in Table VIIc. In Fig. 15 Cr, V, Ni, Co and Fe are plotted with respect to the variation in Mg. In each of the linear variation diagrams the vertical scale for the trace elements is exaggerated either 100 or 1000 times as stated in the legends accompanying the text figures.

All the trace elements of the Andean intrusive suite of Graham Land were determined spectrographically by methods identical to those described by Nockolds and Allen (1953). Manganese and titanium were estimated colorimetrically.

The distribution of the trace elements with respect to the major elements is discussed below.

Gallium (Tables VIIb and c; Fig. 11). Since gallium has the same charge as, but a slightly larger ionic radius than, aluminium, it should appear in the aluminous rock-forming minerals camouflaged as aluminium. In this igneous series gallium follows practically the same distribution curve as aluminium, being low in amount in the basic accumulates and at the acid end of the series. This means that there is a greater concentration in the more aluminous or felspar-rich quartz-diorite–basic diorite group, but where quartz is in excess of the felspars in the acid rocks gallium decreases markedly. In this series there is no appreciable fluctuation in the Ga × 1000/Al ratio, the mean of which is 0.25. This is in accord with the results of Nockolds and Allen (1953) and Nockolds and Mitchell (1948), who have found this ratio practically constant.

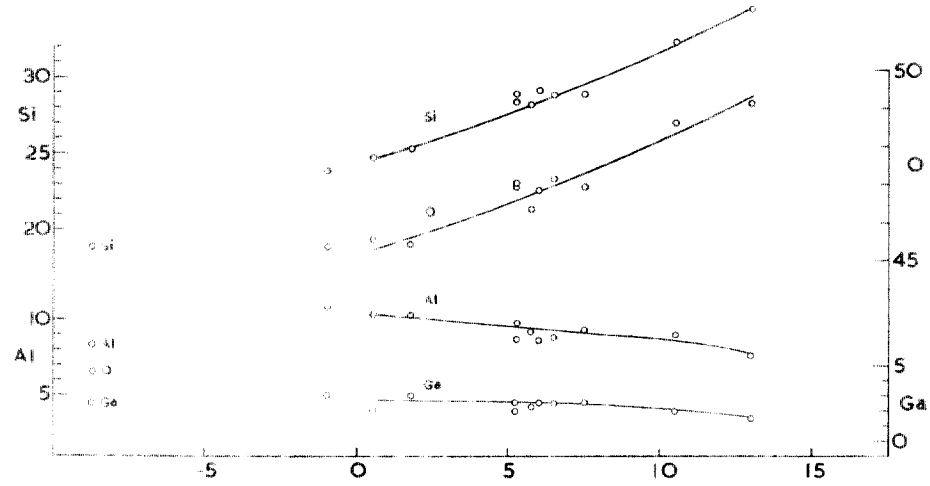

FIGURE 11

Variation diagrams for Si, O, Al (all wt. %) and Ga (wt. % × 1000) plotted against [(1/3Si + K)—(Ca + Mg)].

Chromium (Tables VIIb and c; Figs. 12 and 15). In this series chromium decreases steadily in amount from the basic accumulates to the acid rocks. The distribution curve follows the relatively gradual decrease in the total modal percentages of the ferro-magnesian minerals (including magnetite and ilmenite) throughout the series.

Lithium (Tables VIIb and c; Fig. 12). Lithium has a considerably smaller ionic radius than the alkali ions, sodium and potassium. Its ionic size is almost the same as magnesium but since the charge is smaller than that of magnesium, it should be admitted into magnesian minerals and the more highly ferro-magnesian-rich rocks. A certain amount of lithium enters the magnesian minerals, but as the rocks become more acid the actual amount of lithium increases gradually and quite a considerable quantity of lithium appears to concentrate in the liquid residuum. In the present series there is a definite inverse relation between the distribution of lithium and magnesium, and the Li × 1000/Mg ratio increases steadily towards the acid end of the series.

The distribution of lithium in relation to the chemically similar alkali ions, sodium and potassium, follows a similar trend. All of these elements are relatively more abundant in the granites than in the gabbros.

Cobalt (Tables VIIb and c; Figs. 12 and 15). The cobalt ion is almost the same size as the Fe^{++} ion, so it would naturally be expected that the former would appear concealed in the latter. Excluding the basic

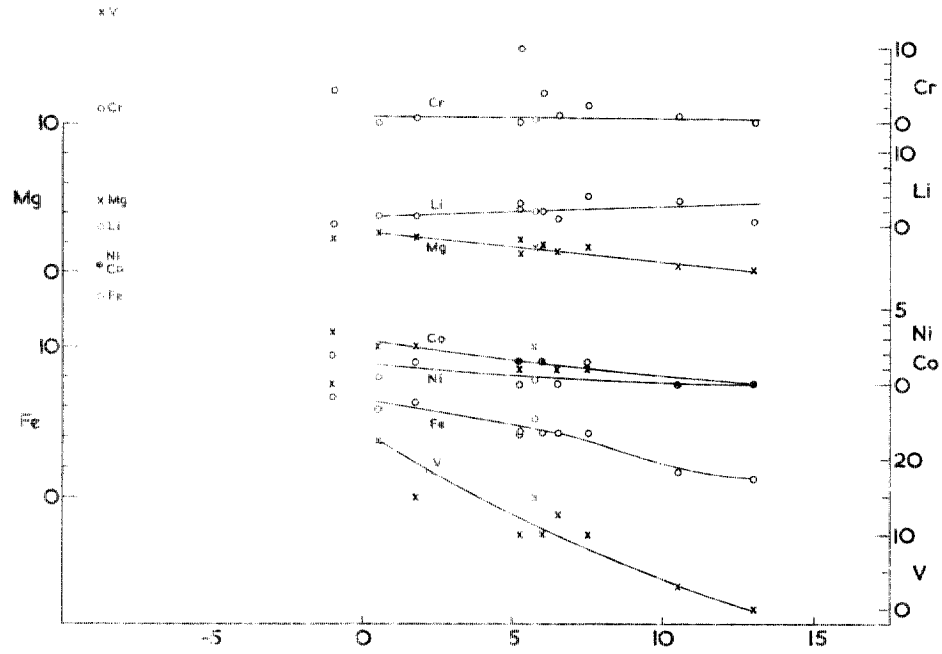

FIGURE 12

Variation diagrams for Cr (wt. % ×1000), Li (wt. % ×1000), Mg (wt. %), Co (wt. % ×1000), Ni (wt. % ×1000), Fe (wt. %) and V (wt. % ×1000) plotted against [(1/3Si+K)—(Ca+Mg)].

accumulates, the Co × 1000/Fe ratio, though showing a slight decrease in the acid rocks, remains practically constant throughout this series and the mean ratio is 0.36. If the effective ionic radius of cobalt is really less than 0.72 Å (Ahrens, 1952), it has a size comparable to that of magnesium. Comparison of Co × 1000/Mg ratios for the series shows a slight decrease as fractionation proceeds towards the acid end. The mean value for this ratio is 0.92, which agrees very closely with that given by Nockolds and Allen (1953).

In the very basic accumulate (olivine-gabbro) shown in Fig. 12, cobalt and nickel both have the same value but in the normal gabbros cobalt is considerably in excess of nickel. This lends support to the suggestion of Mason (1952) that both nickel and cobalt are removed early in the crystallisation process and are fixed in the olivine.

Nickel (Tables VIIb and c; Figs. 12 and 15). Though the actual amount of nickel is always lower than that of cobalt for this series, the Ni/Mg ratio shows a constant decrease with progressive fractionation. This perhaps indicates the withdrawal of nickel together with magnesium in the early stages of crystallisation.

In the Californian Batholith plutonic series, the calc-alkali volcanic series of the East Central Sierra Nevada and the Lesser Antilles volcanic series (Nockolds and Allen, 1953), cobalt is also in excess of nickel, but in the first-mentioned series there is a reversal of the Co/Ni ratio in the more basic rocks.

Vanadium (Tables VIIb and c; Figs. 12 and 15). The amount of vanadium in the Graham Land rocks decreases remarkably rapidly with increasing acidity, being as high as 800 p.p.m. in the olivine-gabbros and almost zero in the granites. Since vanadium does not concentrate in pyroxenes, amphiboles or micas (Mason, 1952) and since all of these minerals abound in the diorites which have a relatively low vanadium content, it must be confined to the iron ores which comprise up to 12% of the modal composition of some of the Terra Firma olivine-gabbros.

The V/Fe ratio decreases towards the acid end of the series, whereas the V/Mg ratio shows some degree of fluctuation in the same direction.

Strontium (Tables VIIb and c; Fig. 13). In the early basic rocks strontium has a relatively small concentration with a low Sr × 100/Ca ratio, but as fractionation proceeds into the diorite range strontium is suddenly withdrawn, probably into the early basic cores of the zoned plagioclase felspars, together with calcium, thus

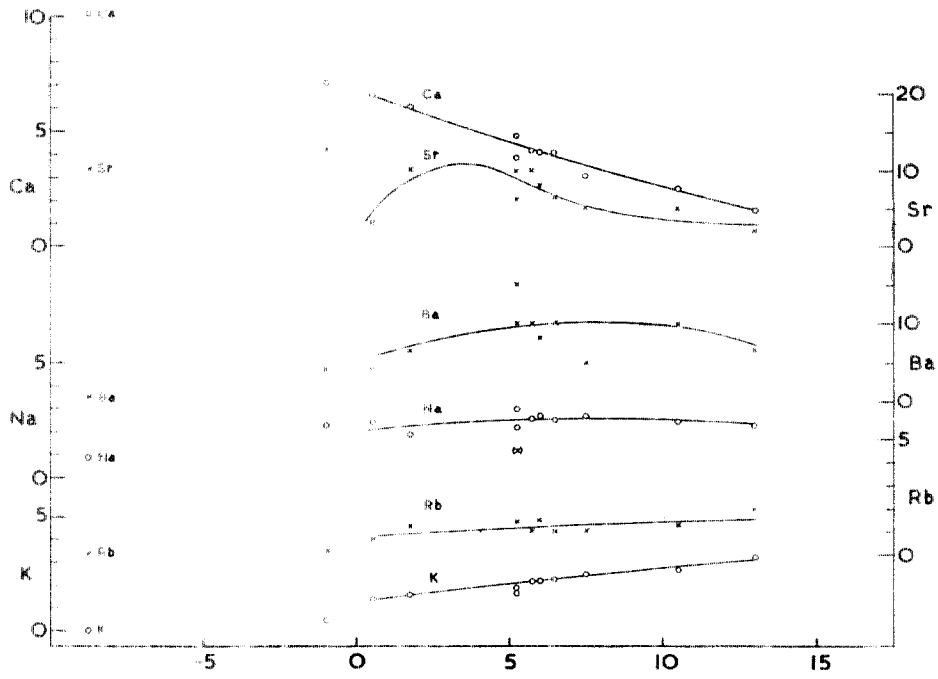

FIGURE 13

Variation diagrams for Ca (wt. %), Sr (wt. % ×100), Ba (wt. % ×100), Na (wt. %), Rb (wt. % ×100) and K (wt. %) plotted against [(1/3Si+K)—(Ca+Mg)].

giving a steep rise in the Sr × 100/Ca ratio. Towards the granite end of the series this ratio decreases gradually from a maximum value. The ratio Sr × 100/Ca+K shows a similar trend. Because the individual minerals have not been separated and analysed, it is not possible to indicate whether there is necessarily any concentration of strontium in early potassic minerals as Nockolds and Mitchell (1948) observed in the Scottish Caledonian series.

Barium (Tables VIIb and c; Fig. 13). Like strontium, which may be taken into early potassic minerals together with potassium, barium has too large an ionic radius to replace either calcium or sodium. Its ionic radius is comparable with that of potassium, and therefore may be taken into biotite or early potash-felspar. In the present series this is apparently so, because barium is found at its highest concentration in the diorite range where biotite first begins to crystallise. The amount of barium decreases steadily as orthoclase forms in the more acid rocks. In the early accumulates (olivine-gabbros) the barium content is negligible. The Ba × 100/K ratio for this series shows a decreasing tendency with increasing acidity.

Rubidium (Tables VIIb and c; Fig. 13). Since its ionic size is much larger than that of potassium, rubidium can only occur as a replacement of potassium in potassic minerals such as biotite and potash-felspar (Mason, 1952). In fact, the rubidium distribution curve follows that of potassium closely. With progressive differentiation there is a slight increase in the Rb × 100/K ratio with the mounting concentration of rubidium in the potash-felspar of the granites. If the abnormally high value for the highly altered quartz-diorite (Table VIIb, No. 8) is neglected, the average Rb × 100/K ratio is 0.57. Nockolds and Allen (1953) found an average value of 0.61 for this ratio in the East Central Sierra Nevada andesite–rhyolite series, but for series deficient in potassium (Crater Lake and the Lesser Antilles) this ratio was as low as 0.28 and 0.36 respectively.

Zirconium (Table VIIb; Fig. 14). Zirconium can occur as zircon and in the ferro-magnesian minerals of igneous rocks. It would seem that during the course of progressive crystallisation the greater part of the zirconium is withdrawn at the biotite-diorite stage and decreases steadily in amount until the concentration

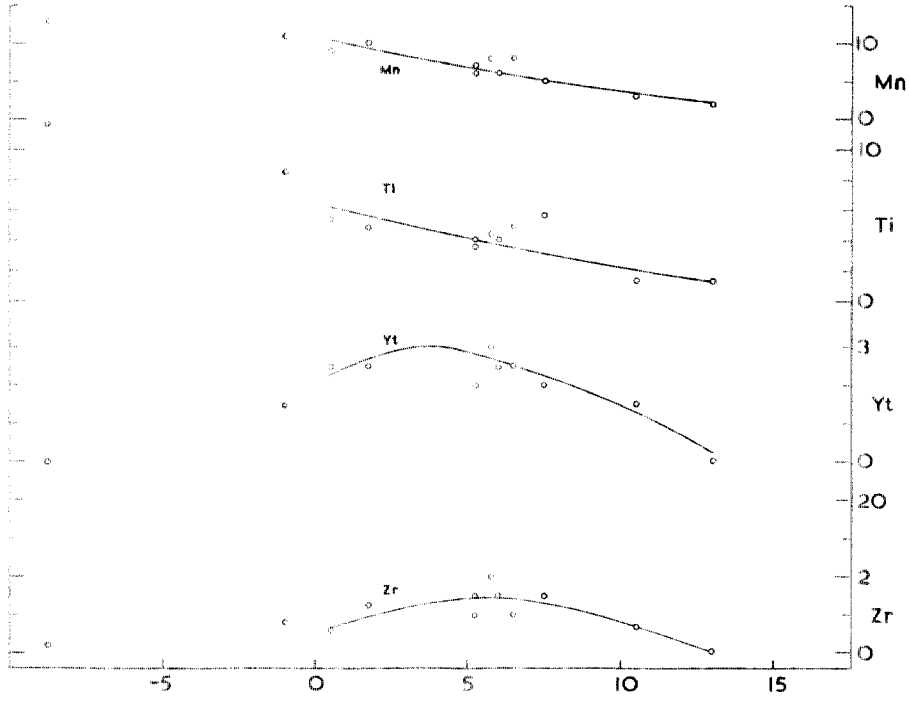

FIGURE 14
Variation diagrams for Mn (wt. % ×100), Ti (wt. % ×10), Y (wt. % ×1000) and Zr (wt. % ×100) plotted against [(1/3Si+K)—(Ca+Mg)].

in the granites is small, being represented here by zircon alone. In the mineralogical composition of these rocks this fact is particularly noticeable, as there is far less modal zircon in the granites than in the biotite- and amphibole-diorites.

Yttrium (Tables VIIb and c; Fig. 14). In actual amount, yttrium has its greatest concentration in the diorites, which contain a high percentage of titanite. It is possible that yttrium has entered the titanite and has been withdrawn at a comparatively early stage of differentiation. The ratio Y × 1000/Ca rises regularly to a maximum then decreases slightly in the most acid rocks.

Scandium, Lead and Molybdenum (Table VIIb). Whereas scandium has been found in amounts above the limit of sensitivity (10 p.p.m.) only in the very basic rocks, lead seems to occur only in the most acid diorites and granites. Molybdenum exceeds the limit of sensitivity (2 p.p.m.) in only one of the quartz-biotite-diorites (Table VIIb, No. 6).

Lanthanum, Caesium, Thallium, Beryllium and Boron (Table VIIb). In this series lanthanum, caesium, thallium and beryllium do not exceed their limits of sensitivity (40, 15, 2 and 5 p.p.m. respectively). Boron was not determined.

Titanium (Table VIIb; Fig. 14). Since much of the titanium in these rocks probably occurs as ilmenite and titanite rather than in the ferro-magnesian silicates, it is not surprising to find high concentrations (up to 1.2% Ti) in the early accumulates. The amount of titanium decreases regularly to traces in the acid differentiates.

Manganese (Table VIIb; Fig. 14). Both Mg^{+2} and Fe^{+2} can be replaced by manganese, particularly in the ferro-magnesian minerals. The Mn/Fe ratio remains fairly constant throughout this series, indicating that manganese is withdrawn from the parent magma proportionally to the amount of iron. Nockolds and Mitchell (1948), in their investigation of the Scottish Caledonian plutonic series, observed that the Mn/Fe ratio showed an increase in the later differentiates.

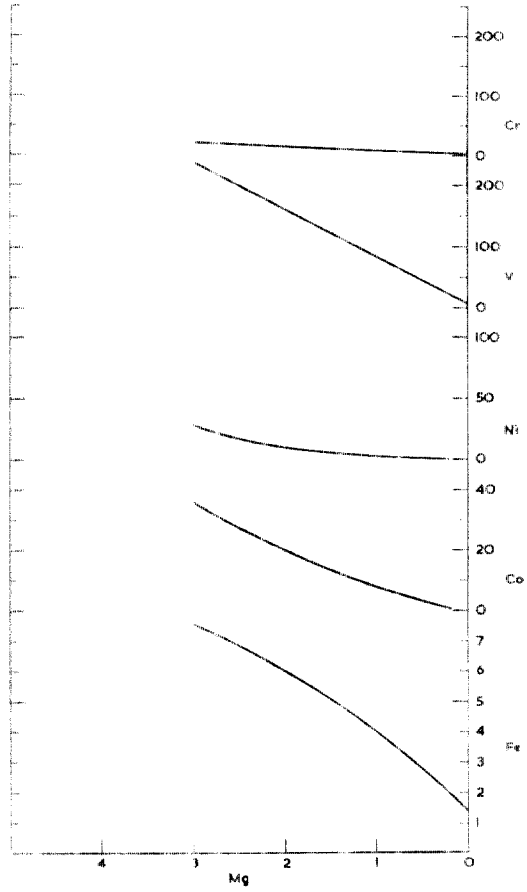

FIGURE 15

Variation diagrams for Cr, V, Ni, Co and Fe with respect to Mg. Values for trace elements in p.p.m.; values for Fe and Mg in weight per cent.

Phosphorus (Table VIIb). The somewhat erratic results obtained by the gravimetric estimation of phosphorus may be due to the method of determination. For igneous rocks containing less than 0.5% of P_2O_5 it is now considered preferable to determine this constituent colorimetrically.

The general distribution of the trace elements in the Graham Land granite–gabbro series bears the closest resemblance to that described by Nockolds and Allen (1953) for the calc-alkali volcanic series of the East Central Sierra Nevada. It is, however, unfortunate that such a small number of results are at present available for this discussion and that the extremely acid types, the pegmatites and aplites, have not yet been analysed.

This igneous differentiation series is associated with the Andean orogeny. In view of this fact, it is not at all surprising to find that both the major and trace element distribution trends follow closely those of a normal calc-alkali differentiation series. In this respect, these results may also be compared to some extent with those for the Californian Batholith (Nockolds and Allen, 1953) and the Scottish Caledonian plutonics (Nockolds and Mitchell, 1948; Nockolds and Allen, 1953).

3. The Parental Magma

From the diagrammatic interpretation of the new analytical data (Figs. 10 to 14) it is possible to obtain an approximation of the chemical composition of the parental magma of this series. In Figs. 9 and 10 it is

clear that on both sets of co-ordinates the majority of the rocks lie on smooth curves, but at the basic end of both curves there is considerable scattering of the rock positions. These rocks are interpreted as early basic accumulates of the parental magma. The rocks that fall on the smooth curves are thought to represent later differentiates on the *same* line of liquid descent from the *same melt*. The plotted position of the supposed parental magma would therefore lie at the basic end of the smooth curves as is indicated in the triangular variation diagram (Fig. 10). For the present series the approximate chemical composition of the parental magma, given in Table VIII, is believed to be close to the mean of Nos. 3 and 4 in Tables VIIa, b and c.

TABLE VIII

APPROXIMATE CHEMICAL COMPOSITION OF THE PARENTAL MAGMA OF THE ANDEAN GRANITE-GABBRO INTRUSIVE SUITE OF GRAHAM LAND

(see Fig. 10)

	Wt. %		p.p.m.		p.p.m.*			
SiO_2	53.56	Si^{+4}	$250 \cdot 10^3$	Ga^{+3}	30	*Norm*		
TiO_2	0.86	Ti^{+4}	$5 \cdot 10^3$	Cr^{+3}	10	Q	3.36	
Al_2O_3	19.48	Al^{+3}	$103 \cdot 10^3$	V^{+3}	200	or	10.56	
Fe_2O_3	1.67	Fe^{+3}	$12 \cdot 10^3$	Li^{+1}	15	ab	24.63	
FeO	6.29	Fe^{+2}	$49 \cdot 10^3$	Ni^{+2}	15	an	34.75	
MnO	0.13	Mn^{+2}	$1 \cdot 10^3$	Co^{+2}	25	$CaSiO_3$	2.55	di 5.04
MgO	4.06	Mg^{+2}	$25 \cdot 10^3$	Y^{+3}	25	$MgSiO_3$	10.20	hy 16.56
CaO	8.84	Ca^{+2}	$63 \cdot 10^3$	Sr^{+2}	650	$FeSiO_3$	8.85	
Na_2O	2.87	Na^{+1}	$22 \cdot 10^3$	Ba^{+2}	600	mt	2.55	
K_2O	1.83	K^{+1}	$15 \cdot 10^3$	Rb^{+1}	75	il	1.67	
P_2O_5	0.41	P^{+5}	$2 \cdot 10^3$	Zr^{+4}	90	ap	1.01	

Position		[(1/3Si+K)−(Ca+Mg)]		+1.0	
Fe	71	Fe	50	Ca	63
Mg	29	Mg	20	Na	22
		Alk	30	K	15

*All trace element values are extrapolated from the variation diagrams.

A comparison of the chemical composition of the parental magma of the Graham Land Andean intrusive suite (Table VIII) with the parental magma compositions of the ten calc-alkali series discussed by Nockolds and Allen (1953, Tables 8 and 9) reveals that the present series is chemically closest to the normal calc-alkali pyroxene-andesite-rhyolite series of the East Central Sierra Nevada. There is close agreement not only in the major elements but also in the trace elements. A point worthy of special mention is that in both these series the amount of cobalt exceeds that of nickel, whereas in the majority of the calc-alkali series described the reverse is the case. For the Graham Land series the Fe : Mg ratio is 71 : 29, which is the same as that for the East Central Sierra Nevada series.

Here an intrusive series is being compared chemically with one of a volcanic origin. It is, therefore, interesting to note that though the rocks of these two series have a vastly different mode of occurrence (batholithic emplacement and extrusion), their chemical behaviour is similar.

GEOCHEMISTRY OF THE ANDEAN INTRUSIVE SUITE OF PATAGONIA

THE only available analyses of Andean intrusives from Patagonia (Table IX) were carried out some years ago. For the purpose of comparison with the Graham Land suite they are now recalculated on a water-free basis and plotted on triangular variation diagrams (Fig. 16) with the same co-ordinates as in Fig. 9.

TABLE IX

PREVIOUS CHEMICAL ANALYSES OF THE ANDEAN INTRUSIVE SUITE OF PATAGONIA

	1	2	3	4	5	6	7	8	9	10	
SiO_2	45.18	48.76	49.30	52.50	59.06	60.13	60.35	68.0	68.32	69.43	SiO_2
TiO_2	2.00	0.54	2.16	0.62	—	—	0.73	—	0.31	—	TiO_2
Al_2O_3	14.69	21.41	17.31	16.02	16.79	17.49	18.95	15.6	15.41	15.74	Al_2O_3
Fe_2O_3	1.94		3.84	1.70	3.47	2.89	—	—	—	0.93	Fe_2O_3
FeO	8.93	7.92*	5.73	6.58	4.83	3.35	5.23*	5.1*	4.13*	3.35	FeO
MnO	0.16	—	0.14	0.15	—	—	—	—	—	—	MnO
MgO	8.98	4.28	5.12	8.70	3.00	5.30	2.41	0.8	1.37	1.35	MgO
CaO	9.36	12.37	8.67	10.18	5.23	3.72	6.28	2.6	4.83	2.07	CaO
Na_2O	3.14	3.11	4.05	2.34	4.60	4.42	3.50	4.6	3.02	4.56	Na_2O
K_2O	0.94	0.65	1.73	1.08	2.79	3.02	0.45	2.7	1.80	2.99	K_2O
H_2O+	3.80	0.49	2.18	0.19	0.95	1.04	0.96	—	0.25	0.10	H_2O+
H_2O-				—	—	—	—	—	—	—	H_2O-
CO_2	0.32		0.16	—		—	—	—	—	—	CO_2
P_2O_5	0.35	—	0.26	0.11	—	—	—	—	—	—	P_2O_5
S	0.20	—	0.01	—	—	—	—	—	—	—	S
BaO	0.03	—	—	0.02	—	—	—	—	—	—	BaO
Cr_2O_3	—	—	—	0.05	—	—	—	—	—	—	Cr_2O_3
TOTAL	100.02	100.03	100.66	100.24	100.69	101.36	98.16	99.4	99.44	100.52	TOTAL

*Fe_2O_3 and FeO determined as FeO

1. Essexite-gabbro, Rio Pinto. (Quensel, 1912)
2. Uralitised hornblende-gabbro, Puerto Angosto. (Bodman, 1916)
3. "Essexite", Cerro Cagual. (Quensel, 1912)
4. Bronzite-orthoclase-gabbro, Cerro Payne. (Quensel, 1912)
5. Quartz-bearing andendiorite, San Antoniotal. (Stelzner, 1885)
6. Quartz-bearing andendiorite, Yuncantal. (Stelzner, 1885)
7. Quartz-diorite, Hoste Island. (Bodman, 1916)
8. Granite, Puerto Angosto. (Nordenskjöld, 1905b)
9. Quartz-mica-diorite, Quarenta Dias. (Bodman, 1916)
10. Andengranite (hornblende-bearing biotite-granite), Yuncantal. (Stelzner, 1885)

An inspection of both these triangular variation diagrams (Figs. 9 and 16) reveals that the plot ($FeO+Fe_2O_3$) – – Alk – – MgO for the Patagonian suite follows identically the curve for the Graham Land intrusives using the same co-ordinates (Fig. 9). However, in considering the distribution curve on the co-ordinates K_2O – – Na_2O – – CaO, there is some discrepancy between the Patagonian and Graham Land series. The curve given by the Patagonian rocks, though similar in slope and shape to that for the Graham Land rocks, is

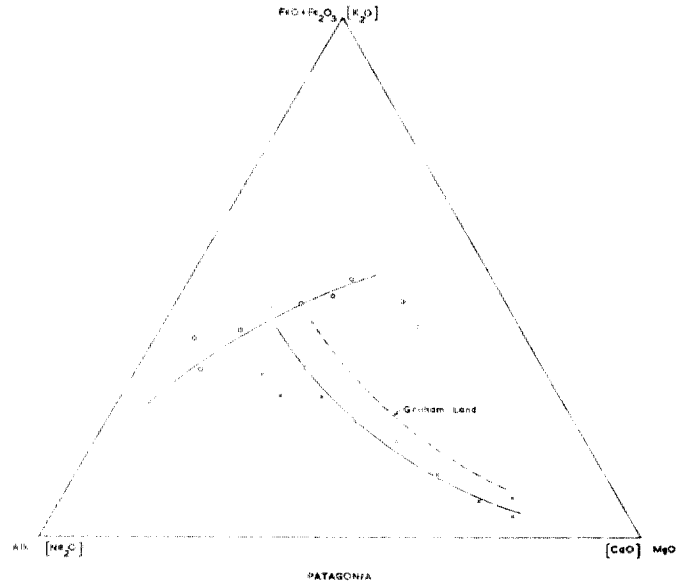

FIGURE 16
Variation diagrams (FeO + Fe_2O_3) – – Alk – – MgO and K_2O – – Na_2O – – CaO for Andean intrusives from Patagonia.

displaced towards Na_2O. In the light of this fact, a re-examination of the distribution of the Graham Land rocks in Fig. 9, on the same co-ordinates, shows that a large number of the earlier analyses have a similar displacement towards Na_2O, although there is no marked discrepancy in the (FeO + Fe_2O_3) – – Alk – – MgO plot.

This possibly indicates that the earlier determinations of the individual alkalis were unreliable. Total alkalis seem to have been correctly estimated and the fault appears to lie in the separation of K_2O from Na_2O, the determination of the latter being too high.

SUMMARY

IN the past several authors have put forward hypotheses concerning the relationship between the early Tertiary intrusive rocks of the western Patagonian cordillera and Graham Land. From a cursory petrographic study of an assortment of rocks from both these regions, Nordenskjöld (1905a and 1910) reached the conclusion that the respective igneous assemblages of the two areas were genetically connected. This theory was pursued more deeply by Bodman (1916), who supported his similar conclusion with detailed petrography and a number of chemical analyses. The South American igneous rocks with which he compared his Graham Land material were selected somewhat at random and recent careful examination of their petrography has shown that some of the acid rocks used by Bodman in his comparison are in fact much earlier in age than the Andean intrusives.

Barth and Holmsen (1939) have superficially investigated this problem, supporting their complete argument for a migmatitic or palingenic origin of the Andean granite–gabbro intrusive suite of Graham Land with four analyses. In discussing the composition of the intrusives, they claim that earlier volcanics (presumably of Upper Jurassic age) are the chief contaminant of the intrusives. Though a certain degree of contamination of the intrusives is known to occur within the Graham Land area, it is not of such great significance as supposed by Barth and Holmsen.

In the foregoing pages, field occurrence, petrography and geochemistry of the Andean intrusives of Graham Land have been considered.

On the triangular variation diagrams (Figs. 9 and 10) geochemical data for the very basic gabbros show scattering, but those for the normal gabbro–granite series fall on smooth curves. The former rocks are

accordingly interpreted as *basic accumulates* whereas the latter are believed *to lie on the same line of liquid descent* from the *parental magma*. On the plots showing variation in the individual elements (Figs. 11 to 14) with respect to the function [(1/3Si+K)−(Ca+Mg)], both the major and trace elements of the very basic (i.e. accumulative) rocks exhibit deviations and scattering and there is a certain degree of iron enrichment, but those of the other members of the series follow smooth and regular curves (i.e. lie on the same line of liquid descent).

As far as has been possible with the limited analytical data, the Patagonian Andean series is compared geochemically with that of Graham Land.

The data given above are further evidence that the Andean granite–gabbro intrusive suite of Graham Land is a normal calc-alkali magmatic series, having been derived by a crystallisation-differentiation process from a common parental magma, the approximate chemical composition of which is given in Table VIII.

ACKNOWLEDGMENTS

THANKS are due to Dr. V. E. Fuchs, in whose company most of the field work was carried out, for helpful advice and for allowing the use of his field sketches (Figs. 5 and 6). Dr. S. R. Nockolds and Mr. R. Allen of the Mineralogy and Petrology Department, Cambridge, very kindly determined the trace elements given in Table VIIb. The guidance and encouragement of Dr. S. R. Nockolds are gratefully acknowledged. I am also indebted to two former colleagues, Surgeon Lieutenant-Commander D. G. Dalgliesh and Major R. E. Spivey, for placing at my disposal their field observations and specimens collected in northern Marguerite Bay. To my wife, who prepared the greater part of the manuscript for publication, I wish to express my gratitude.

REFERENCES

AHRENS, L. H. 1952. The Use of Ionisation Potentials. Part I. Ionic Radii of the Elements, *Geochim. et Cosmoch. Acta*, **2**, No. 3, 155–69.

BARTH, T. F. W. and P. HOLMSEN. 1939. Rocks from the Antarctandes and the Southern Antilles. Being a description of rock samples collected by Olaf Holtedahl 1927–28, and a discussion of their mode of origin, *Sci. Res. Norweg. antarct. Exped.*, No. 18, 64 pp.

BARTH, T. F. W. 1940. Notes on Igneous and Palingenic Rocks from the Antarctic Archipelago. A contribution to the petrology of circum-Pacific rock types. *Proc. Sixth Pacific Sci. Congress* (1939), **2**, 747–54.

BODMAN, G. 1916. Petrographische Studien über einige antarktische gesteine, *Wiss. Ergebn. schwed. Südpolarexped.*, 1901–3, Bd. 3, Lief 15, 1–100.

ELLSWORTH, L. 1937. The First Crossing of Antarctica, *Geogr. J.*, **89**, No. 3, 193–213.

FERGUSON, D. 1921. Geological Observations in the South Shetlands, the Palmer Archipelago, and Graham Land, Antarctica, *Trans. roy. Soc. Edinb.*, **53**, Part 1, No. 3, 29–55.

FUCHS, V. E. 1953. Organisation and Methods. *Falkland Islands Dependencies Survey Scientific Reports*, No. 1, 12 pp.

GOURDON, E. 1905. Les roches éruptives grenues de la Terre de Graham recueillies par l'expédition antarctique du Dr. Charcot, *C.R. Acad. Sci. Paris*, **141**, No. 24, 1036–8.

———, 1906. Les roches microlithiques de la Terre de Graham recueillies par l'expédition antarctique du Dr. Charcot, *C.R. Acad. Sci. Paris*, **143**, No. 3, 178–80.

———, 1907. Sur un microgranite alcalin recueilli sur la Terre de Graham par l'expédition antarctique du Dr. Charcot, *C.R. Acad. Sci. Paris*, **144**, No. 22, 1224–6.

———, 1908. *Géographie physique, Glaciologie, Pétrographie des régions visitées par l'Expédition Antarctique Française commandée par le Dr. Charcot*, 1903–5, 214 pp., Paris.

———, 1917. *Minéralogie, Géologie: Deuxième Expédition Antarctique Française* (1908–10) *commandée par le Dr. Charcot*, 1–10, Paris.

———, 1919. Relacion de los trabajos de geología y glaciología, ejecutados en la Antártida por la misión a orden del Doctor Charcot (1908–10). *Bol. Inst. geogr. argent.*, **24**, 128–38.

HACKMAN, V. 1905. Die chemische Beschaffenheit von Eruptivgesteinen Finnlands und der Halbinsel Kola im Lichte des neuen Amerikanischen systemes, *Bull. Comm. géol. Finl.*, No. 15, 59.

HAUTHAL, H. 1898. Ueber patagonisches Tertiär, *z. Dtsch. geol. Ges.*, **50**, 436–40.

HOLTEDAHL, O. 1929. On the Geology and Physiography of Some Antarctic and Sub-antarctic Islands, *Sci. Res. Norweg. antarct. Exped.*, No. 3, 172 pp.

JARDINE, D. 1950. Geological Report on King George Island, 1949–50. Falkland Islands Dependencies Scientific Bureau unpublished report No. 83/50.

KNOWLES, P. H. 1945. Geology of Southern Palmer Peninsula, Antarctica, *Proc. Amer. phil. Soc.*, **89**, 132–45.

MASON, B. 1952. *Principles of Geochemistry*, John Wiley and Sons, New York.

NICHOLS, R. L. 1948. Preliminary Report on the Geology of the Marguerite Bay Area, Antarctica, *Ronne Antarctic Research Expedition Technical Report*, No. 6, 5 pp.

NOCKOLDS, S. R. and R. L. MITCHELL. 1948. The Geochemistry of Some Caledonian Plutonic Rocks: a study in the relationship between the major and trace elements of igneous rocks and their minerals, *Trans. roy. Soc. Edinb.*, **61**, 533–75.

———— and R. ALLEN. 1953. The Geochemistry of Some Igneous Rocks, *Geochim. et Cosmoch. Acta*, **4**, 105–42.

NORDENSKJÖLD, O. 1905a. Petrographische Untersuchungen aus dem westantarktischen Gebiete, *Bull. geol. Instn. Univ. Upsala*, **6**, Part 2, 234–46.

————. 1905b. Die krystallinischen Gesteine der Magellansländer, *Wiss. Ergebn. schwed. Exped. Magell.*, 1895–7, Bd. 1, Lief 6, 175–240.

————. 1910. Die geologischen Beziehungen zwischen Südamerika und der angrenzenden Antarktika, *C.R. 11th Congr. Geol. Internat., Stockholm*, 759–65.

PELIKAN, A. 1909. Petrographische Untersuchung der Gesteinsproben, *Expédition Antarctique Belge. Résultats du Voyage du S.Y. Belgica, en* 1897–1898–1899, *Rapports scientifiques, géologie*, Teil I, 1–49.

QUENSEL, P. D. 1912. Geologisch-petrologische Studien in der Patagonischen Cordillera, *Bull. geol. Instn. Univ. Upsala*, **11**, 1–114.

REID, J. A. 1902. The Igneous Rocks near Pajaro, *Bull. Dept. Geol. Univ. Calif.*, **3**, 176–9.

SISTEK, D. 1912. Petrographische Untersuchungen der Gesteinsproben, *Expédition Antarctique Belge. Résultats du Voyage du S.Y. Belgica, en* 1897–1898–1899, *Rapports scientifiques, géologie*, Teil II, 1–20.

STELZNER, A. 1885. *Beiträge zur Geologie und Palaeontologie der Argentinischen Republik*, 329 pp., Berlin.

TYRRELL, G. W. 1921. A Contribution to the Petrography of the South Shetland Islands, the Palmer Archipelago, and the Danco Land Coast, Graham Land, Antarctica, *Trans. roy. Soc. Edinb.*, **53**, Part 1, 57–79.

————. 1945. Report on Rocks from West Antarctica and the Scotia Arc, '*Discovery*' *Rep.*, **23**, 37–102.

VAN HORN, F. R. 1897. Petrographische Untersuchungen über die noritischen Gesteine der Umgegend von Ivrea in Oberitalien, *Miner. petrogr. Mitt.*, **17**, 414.

APPENDIX

A LIST OF PLACE-NAMES, THEIR CO-ORDINATES AND THE APPROPRIATE MAP SHEETS

NOTE: Only the mid latitude and longitude of each feature is given.
Names which are not yet officially accepted are printed in inverted commas.

Adams, Cape	75°04′S., 62°20′W.	1/200,000 Sheet 74 62
Adelaide Island	67°15′S., 68°30′W.	1/500,000 Sheet D.
Alamode Island	68°43′S., 67°32′W.	1/200,000 Sheet 68 66
Alexander Land	72°00′S., 70°00′W.	1/500,000 Sheets F, G & K.
Anna, Cape	64°36′S., 62°27′W.	1/200,000 Sheet 64 62
Anvers Island	64°35′S., 63°30′W.	1/200,000 Sheets 64 62, 64 64
Barn Rock	68°42′S., 67°33′W.	1/200,000 Sheet 68 66
Berteaux, Cape	68°51′S., 67°29′W.	1/200,000 Sheet 68 66
Berthelot Islets	65°20′S., 64°09′W.	1/200,000 Sheet 65 64
Biscoe Islands	65°45′S., 66°15′W.	1/500,000 Sheet C.
Black Coast	71°40′S., 61°00′W.	1/500,000 Sheets H & L.
Black Thumb Mountain	68°25′S., 66°53′W.	1/200,000 Sheet 68 66
Blade Ridge	63°25′S., 57°05′W.	1/100,000 Sheet 63 56 NW.
Booth Island	65°05′S., 64°00′W.	1/200,000 Sheets 65 62, 65 64
Borchgrevink Nunatak	66°03′S., 62°30′W.	1/200,000 Sheet 66 62
Bowman Coast	68°15′S., 65°30′W.	1/500,000 Sheets C & G.
Brabant Island	64°15′S., 62°20′W.	1/200,000 Sheets 63 62, 64 60, 64 62
Bransfield, Mount	63°17′S., 57°06′W.	1/100,000 Sheet 63 56 NW.
Brown Bluff	63°32′S., 56°55′W.	1/100,000 Sheet 63 56 SE.
Bryant, Cape	71°12′S., 60°55′W.	1/200,000 Sheet 71 60
Bulcke, Mount	64°28′S., 62°39′W.	1/200,000 Sheet 64 62
Buttress Nunataks	72°22′S., 66°47′W.	1/200,000 Sheet 72 66
Calmette, Cape	68°04′S., 67°14′W.	1/200,000 Sheet 68 66
Camp Point	67°58′S., 67°19′W.	1/200,000 Sheet 67 66
Carisimo, Cape	72°20′S., 60°41′W.	1/200,000 Sheet 72 60
Compass Islet	68°38′S., 67°48′W.	1/200,000 Sheet 68 66
Darco Coast	64°45′S., 62°00′W.	1/500,000 Sheet A
Depot Glacier	63°25′S., 57°03′W.	1/100,000 Sheet 63 56 NW.
Dumbbell Islet	68°43′S., 67°34′W.	1/200,000 Sheet 68 66
Fielson Peninsula	70°37′S., 61°52′W.	1/200,000 Sheets 70 60, 70 62
Fiskund Islands	72°16′S., 72°07′W.	1/200,000 Sheets 73 72, 73 73
Evensen Nunatak	64°59′S., 60°25′W.	1/200,000 Sheet 64 60
Falleres Coast	67°55′S., 66°45′W.	1/500,000 Sheet C
Flyspot Rocks	68°35′S., 68°06′W.	1/200,000 Sheet 68 68
Foyn Coast	66°50′S., 64°30′W.	1/500,000 Sheets C & D.
Fridtjof Island	64°53′S., 63°22′W.	1/100,000 Sheet 64 62 SW.
Graham Coast	66°05′S., 65°20′W.	1/500,000 Sheet C
Gulliver Nunatak	66°12′S., 62°40′W.	1/200,000 Sheet 66 62
"Hamilton, Cape"	64°21′S., 57°16′W.	1/100,000 Sheet 64 56 NE.
Hayrick Islet	68°42′S., 67°33′W.	1/200,000 Sheet 68 66
Hope Bay	63°24′S., 57°00′W.	1/100,000 Sheets 63 56 NE, NW.
Hovgaard Island	65°08′S., 64°07′W.	1/200,000 Sheet 65 64
James Ross Island	64°05′S., 57°45′W.	1/500,000 Sheet B.
Jenny Island	67°44′S., 68°25′W.	1/200,000 Sheet 67 68
King George VI Sound	71°00′S., 68°00′W.	1/500,000 Sheets G & K.
King Oscar II Coast	65°50′S., 62°20′W.	1/500,000 Sheet D
Last Hill	63°28′S., 57°05′W.	1/100,000 Sheet 63 56 NW.
Laubeuf Fjord	67°30′S., 67°50′W.	1/500,000 Sheet C

Léonie Islands	67°36′S., 68°17′W.	1/200,000 Sheet 67 68
Lizard Hill	63°31′S., 57°01′W.	1/100,000 Sheet 63 56 SW.
Lockroy, Port	64°49′S., 63°30′W.	1/100,000 Sheet 64 62 SW.
Lodge Rock	68°42′S., 67°33′W.	1/200,000 Sheet 68 66
Longridge Head	67°28′S., 67°38′W.	1/200,000 Sheet 67 66
Loubet Coast	66°50′S., 65°55′W.	1/500,000 Sheet C.
Marguerite Bay	68°30′S., 69°00′W.	1/500,000 Sheet G.
Millerand Island	68°09′S., 67°13′W.	1/200,000 Sheet 68 66
Mineral Hill	63°29′S., 57°03′W.	1/100,000 Sheet 63 56 NW.
Moraine Cove	68°35′S., 67°07′W.	1/200,000 Sheet 68 66
Moreno Island	64°03′S., 61°15′W.	1/200,000 Sheet 64 60
Neny Fjord	68°16′S., 66°50′W.	1/200,000 Sheet 68 66
Nobby Nunatak	63°25′S., 56°59′W.	1/100,000 Sheet 63 56 NE.
Nordenskjöld Coast	64°39′S., 60°00′W.	1/500,000 Sheet A.
Palmer Archipelago	64°20′S., 63°00′W.	1/500,000 Sheet A.
Palmer Coast	64°00′S., 60°30′W.	1/500,000 Sheet A.
Petermann Island	65°11′S., 64°11′W.	1/200,000 Sheet 65 64
Pigny Rock	68°43′S., 67°33′W.	1/200,000 Sheet 68 66
Pyramid, The	63°26′S., 57°01′W.	1/100,000 Sheet 63 56 NW.
Red Rock Ridge	68°18′S., 67°05′W.	1/100,000 Sheet 68 66 NW.
Reece, Mount	63°50′S., 58°32′W.	1/500,000 Sheet B.
Refuge Islets	68°21′S., 67°10′W.	1/200,000 Sheet 68 66
Robinson, Cape	66°52′S., 63°43′W.	1/200,000 Sheet 66 62
Roquemaurel, Cape	63°33′S., 58°56′W.	1/100,000 Sheet 63 58 SE.
Snow Hill Island	64°26′S., 57°10′W.	1/500,000 Sheet B.
South Shetland Islands	62°00′S., 58°00′W.	1/500,000 Sheets A & B.
Spire, The	68°18′S., 66°53′W.	1/200,000 Sheet 68 66
Tabarin Peninsula	63°30′S., 57°00′W.	1/100,000 Sheets 63 56 NE, NW, SE, SW.
Taylor, Mount	63°26′S., 57°07′W.	1/100,000 Sheet 63 56 NW.
Terra Firma Islands	68°42′S., 67°32′W.	1/200,000 Sheet 68 66
Three Slice Nunatak	68°02′S., 64°58′W.	1/200,000 Sheet 68 64
Trinity Peninsula	63°30′S., 58°00′W.	1/500,000 Sheet B.
Tuxen, Cape	65°16′S., 64°08′W.	1/200,000 Sheet 65 64
Twig Rock	68°42′S., 67°33′W.	1/200,000 Sheet 68 66
Twin Peaks	63°24′S., 57°07′W.	1/100,000 Sheet 63 56 NW.
Two Hummock Island	64°08′S., 61°40′W.	1/200,000 Sheet 64 60
Webb Island	67°27′S., 67°57′W.	1/200,000 Sheet 67 66
Wiencke Island	64°50′S., 63°25′W.	1/100,000 Sheet 64 62 SW.

Printed in Great Britain under the authority of Her Majesty's Stationery Office by Benham and Company Limited, Colchester
Wt. P25733 K.4 1066 9/55

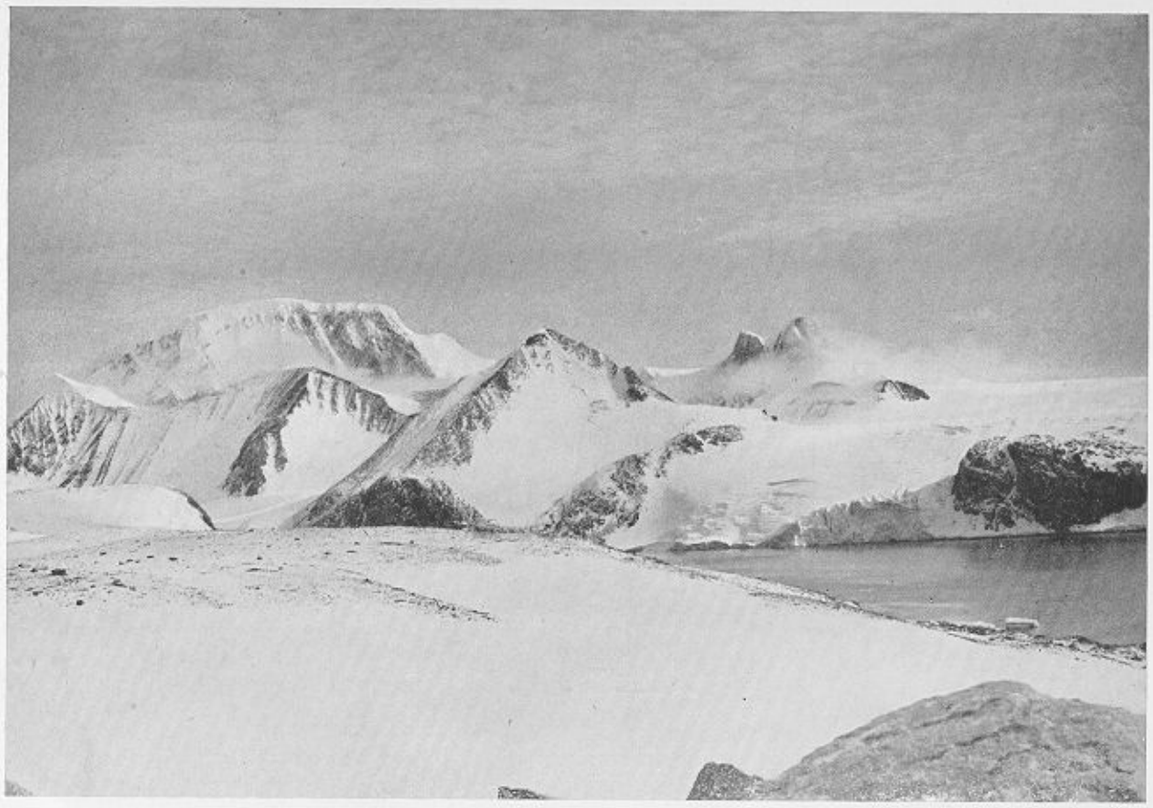

R.J.A.

a

b

R.J.A.

c

a. The Andean quartz-diorite intrusion of Blade Ridge, Hope Bay, Trinity Peninsula. Mount Taylor (left) and Twin Peaks (right) lie behind Blade Ridge.

b. Red Rock Ridge granite, showing its characteristic myrmekitic texture; outcrop beneath The Spire, south side of Neny Fjord, Marguerite Bay (E.39.1; X-nicols; ×19).

c. Basement Complex xenoliths in the quartz-diorites of Longridge Head, Laubeuf Fjord.